1

Methods for Extraction of Nanocellulose from Various Sources

Hanieh Kargarzadeh[1], *Michael Ioelovich*[2], *Ishak Ahmad*[1], *Sabu Thomas*[3,4], *and Alain Dufresne*[5,6]

[1] *Faculty of Science and Technology, School of Chemical Sciences and Food Technology, Polymer Research Center (PORCE), Universiti Kebangsan Malaysia (UKM), 43600 Bangi, Selangor, Malaysia*
[2] *Designer Energy Ltd, 2 Bergman Str., Rehovot, 7670504 Israel*
[3] *Mahatma Gandhi University, International and Inter University Centre for Nanoscience and Nanotechnology, Priyadarshini Hills P.O., Kottayam, Kerala 686560, India*
[4] *Mahatma Gandhi University, School of Chemical Sciences, Priyadarshini Hills P.O., Kottayam, Kerala 686560, India*
[5] *Grenoble Institute of Technology (Grenoble INP) - The International School of Paper, Print Media and Biomaterials (Pagora), CS10065, 38402 Saint Martin d'Hères Cedex, France*
[6] *CNRS, LGP2, 38000 Grenoble, France*

Abstract

This chapter describes the chemistry and structure of cellulose fibers and the existing extraction methods for various kinds of nanocellulose (NC), such as cellulose nanofibrils (CNFs), cellulose nanocrystals (CNCs), amorphous nanocellulose (ANC), and cellulose nanoyarn (CNY). Specific conditions for extraction of NC from various natural sources are discussed in detail. The effects of the extraction methods, pretreatments, and conditions on the structure, morphology, and properties of isolated NC are described.

Keywords *natural sources; nanocellulose; extraction methods; extraction conditions; structure; properties*

List of Abbreviations

AGU	anhydroglucose units
$Al(NO_3)_3$	aluminum nitrate
AmimCl	1-allyl-3-methylimidazolium chloride
ANC	amorphous nanocellulose
BC	bacterial cellulose
BmimCl	1-butyl-3-methylimidazolium chloride
$BmimHSO_4$	1-butyl-3-methylimidazolium hydrogen sulfate
$CaCl_2$	calcium chloride

Handbook of Nanocellulose and Cellulose Nanocomposites, First Edition.
Edited by Hanieh Kargarzadeh, Ishak Ahmad, Sabu Thomas, and Alain Dufresne.

CI	crystalline structure of native cellulose
CI	crystallinity index
CMF	cellulose microfibril
CNC	cellulose nanocrystal
CNF	cellulose nanofibril
CNY	cellulose nanoyarn
DMAc	*N,N*-dimethylacetamide
DMSO	dimethyl sulfoxide
DP	degree of polymerization
EPFBF	empty palm fruit bunch fiber
$Fe_2(SO_4)_3$	iron(III) sulfate
$FeCl_2$	iron(II) chloride
$FeCl_3$	ferric chloride
$FeSO_4$	iron(II) sulfate
GL	glycerol
$H_3PW_{12}O_{40}$	solid phosphor-tungsten acid
HA	hydrochloric acid
HIUS	high-intensity ultrasonication
HPH	high-pressure homogenizers
IL	ionic liquid
KCl	potasium chloride
L/*D*	aspect ratios
LiCl	lithium chloride
MCC	microcrystal or microcrystalline cellulose
NaCl	sodium chloride
NC	nanocellulose
NCDs	nanocrystalline nanodomains
NH_3	ammonia
NMMO	*N*-methylmorpholine-*N*-oxide
PA	phosphoric acid
PCL	paracrystalline layer
PEF	local defect
SA	sulfuric acid
TAPPI	Technical Association of the Pulp and Paper Industry
TEM	transition electron microscopy
TEMPO	2,2,6,6-tetramethylpiperidine-1-oxyl radical
W	watt

1.1 Introduction

The depletion of petroleum-based resources and the attendant environmental problems, such as global warming, have stimulated considerable interest in the development of environmentally sustainable materials, which are composed of cellulose, hemicelluloses, and lignin [1–3]. Bio-based plant materials have various advantages, such as renewability, biodegradability, and

environmental friendliness; therefore, they can be used as suitable replacements for petroleum-based materials as a means of overcoming environmental problems.

Cellulose is the most abundant type of renewable organic matter on Earth, with an annual biosynthetic production that is estimated to be over 10^{11} tons [4]. The biosynthesis of cellulose is a very complex phenomenon, and detailed descriptions of the biosynthesis process can be found in the papers of Brown [5], Saxena and Brown [6], and Dufresne [7]. Cellulose is a fascinating and almost inexhaustible sustainable natural polymer that has been used in the form of fiber or its derivatives for thousands of years, for a wide range of materials and products applications.

The unique hierarchical architecture of natural cellulose consisting of nanoscale fibrils and crystallites allows the extraction of the nanoconstituents via mechanical and chemical methods, or through a combination of both of these techniques. Isolated cellulose nanofibrils (CNFs) are long, thin, and flexible formations composed of alternating crystalline and amorphous domains, whereas the obtained cellulose nanocrystals (CNCs) are rod-shaped crystalline particles released after splitting of the amorphous domains. Other types of nanocellulose (NC), such as amorphous nanocellulose (ANC) and cellulose nanoyarn (CNY) or electrospun nanofibers, have also been reported.

NC has recently gained a significant level of attention in the materials community, which does not appear to be waning. It has been the subject of a wide array of research efforts aimed at different applications, because of its availability, renewability, lightweight, nanoscale dimensionality, unique morphology, and its unsurpassed quintessential physical and chemical properties.

This chapter focuses on the extraction methods applicable to obtaining certain types of NC from various cellulosic sources. In addition, the effect of pretreatment and extraction conditions on the morphology and properties of the obtained NC is described. The effect of pretreatment on the energy consumption level during the manufacturing process is also discussed.

1.2 Hierarchical Structure of Natural Fibers

Plant fibers are the main natural sources of cellulose. They are complex biocomposites that are naturally occurring. An elementary plant fiber is a single cell, typically of length ranging from 1 to 50 mm and with a diameter of approximately 10–50 μm. A single fiber is similar to a microscopic hollow tube, wherein the cell wall surrounds a central lumen. The lumen contributes to the water uptake by the plant fiber.

The cell wall of a fiber is composed of an external primary P-wall and an inner secondary S-wall. The thin P-wall (~100–200 nm thick) contains a loose net of microfibrils. The S-wall has a thickness of 3–6 μm and is composed of three layers: S1, S2, and S3 [8–10]. The S1 and S3 layers are nanosized, while the S2 layer has a thickness of approximately 2–5 μm. The dominating S2 layer is composed of a series of helically wound cellulose microfibrils (CMFs), which are orientated under an acute angle (microfibril angle) toward the fiber axis (Figure 1.1).

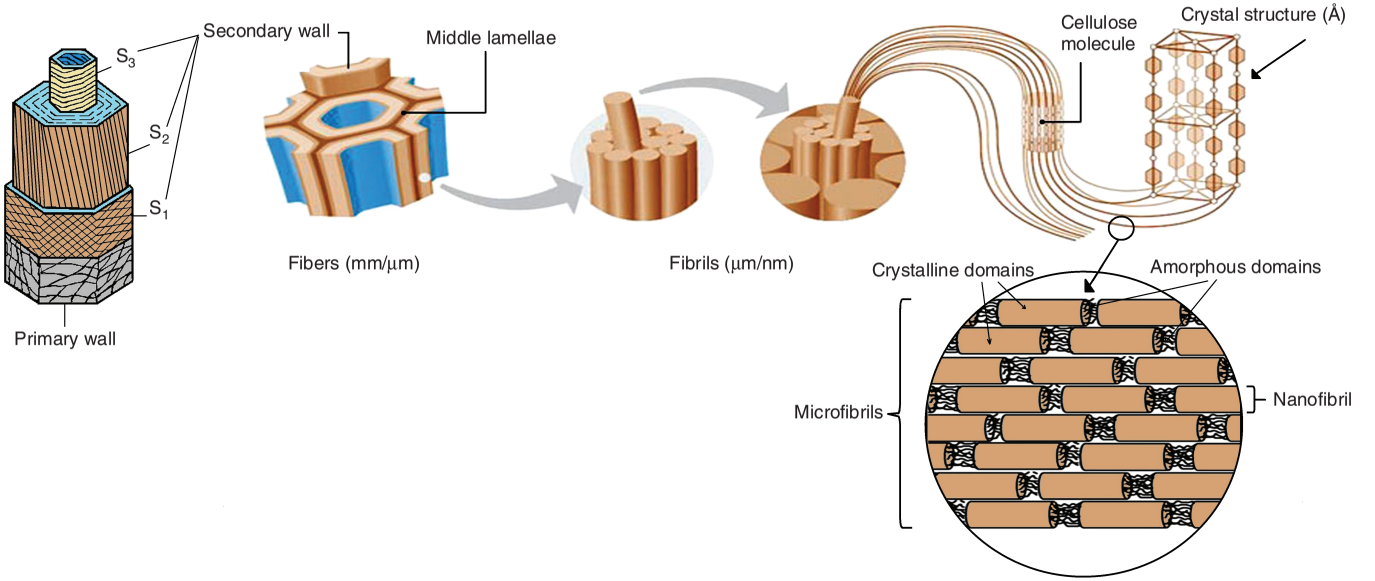

Figure 1.1 Model of cellulose fiber cell wall: S1, S2, and S3 are secondary wall layers; fibril arrangement, microfibrils, and cellulose in plant cell wall; schematic organization of crystalline and amorphous domains in cellulose fiber. (Adapted from [11–13], with permission from Wiley.)

The CMFs of the cell wall reinforce an amorphous matrix consisting of lignin, hemicelluloses, proteins, extractive organic substances, and trace elements. The CMF and hemicelluloses are linked to each other by hydrogen bonds. On the other hand, the hemicelluloses are more strongly linked to lignin through covalent bonds, that is, the hemicellulose component is a compatibilizer between cellulose and lignin. The CMFs with diameter of 10–30 nm are composed of 30–100 cellulose macromolecules in an extended chain conformation.

The structure and chemical composition of plant fiber can vary from one fiber to another and depends on the plant species, age, part, growth area, and climate. This causes considerable variation in fiber characteristics and leads to difficulties in establishing the quality standard [12, 14–16]. The various structures and compositions of plant fibers are responsible for the unique mechanical properties and high strength-to-weight ratio exhibited by plants. However, these characteristics also facilitate flexibility and large dimensional changes due to swelling and shrinking.

1.3 Cellulose Fibers: Structure and Chemistry

Cellulose is a semicrystalline polycarbohydrate composed of anhydroglucose units (AGUs) linked by chemical β-1,4-glycosidic bonds. Two repeating AGUs having a "chair" conformation are shown in Figure 1.2, which also includes the numbering system of carbon atoms. Each such unit contains three hydroxyl functional groups: one primary and two secondary groups. Owing to the equatorial position of the hydroxyls, the AGU can form internal hydrogen bonds, for example, between the hydrogen atom of the C-3 hydroxyl group of one unit and the atom of the ring oxygen of the adjacent units.

The internal hydrogen bonds hinder the free rotation of the glucopyranosic rings around the chemical glycoside bonds, which contributes to increased stiffness of cellulose chains [7]. A strong system of intra- and intermolecular hydrogen bonds of crystallites makes them highly ordered, rigid, and strong cellulose constituents, inaccessible to water and some chemical reagents. On the other hand, very weak hydrogen bonds in noncrystalline amorphous domains contribute to the increased hydrophilicity and accessibility of cellulose materials.

Chemical, physicochemical, and physical modifications of cellulose can lead to changes in its crystalline structure. For instance, as a result of acid hydrolysis,

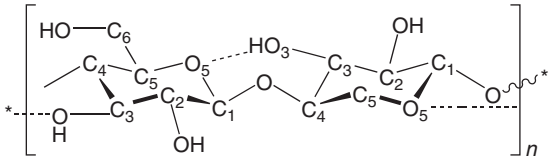

Figure 1.2 Single cellulose chain repeat unit, showing the directionality of the 1–4 linkage and internal hydrogen bonding (dotted line). (Moon *et al.* 2011 [17]. Reproduced with permission of Royal Society of Chemistry.)

part of the noncrystalline domain is removed, yielding cellulose particles with enhanced crystallinity; moreover, some of the released crystallites can cocrystallize and form aggregates with higher lateral sizes [10, 18, 19]. On the other hand, treatment with concentrated alkali, liquid ammonia, or solvents, as well as intensive mechanical grinding, leads to a decrease in crystallite size and crystallinity.

X-ray investigations indicate that cellulose crystallites can occur in four major polymorphic forms: I, II, III, and IV. Mayer and Mish developed the first model of a monoclinic unit cell for the crystalline structure of native cellulose (CI) [20]. This model, which features an antiparallel chain arrangement, was accepted for 30 years, whereupon it was replaced by a more accurate CI model composed of a parallel arrangement of cellulose chains within crystallites [21]. Later, it was found that the CI allomorph can exist in two distinct crystalline forms: I_α containing a triclinic one chain unit cell and I_β containing a monoclinic two chains unit cell [7].

Three additional crystalline allomorphs, II, III, and IV, have been identified, which are attributed to modified celluloses [22, 23]. CII can be obtained through alkaline (AL) treatment of CI, $CIII_1$, $CIII_2$, CIV_1, and CIV_2, as well as by regeneration of cellulose from solutions. The crystalline allomorphs $CIII_1$ and $CIII_2$ can be formed from CI or CIV_1 and CII or CIV_2, respectively, through treatment with liquid ammonia (NH_3). CIV_1 and CIV_2 can be usually obtained through the heating of small crystallites of CI or $CIII_1$ and CII or $CIII_2$ in glycerol (GL) at 260 °C. After treatment of $CIII_1$ and $CIII_2$ with boiling water, these allomorphs recrystallize into CI and CII, respectively. The possible transitions between the various cellulose polymorphs are presented schematically in Figure 1.3.

The shape of the natural cellulose nanocrystallites is a subject of discussion. In several previous studies, the cross-sectional shapes of the crystallites were depicted as squares or rectangles. However, recent studies have shown that the most likely cross-sectional shape of the crystallites of natural cellulose in terraneous plants is a hexagon [18, 24, 25]. Three groups of planes (100), (110), and $(1\bar{1}0)$ are located on the surfaces of CI_β-crystallites, allowing the co-crystallization of adjacent crystallites in different lateral directions [18]. Co-crystallization under isolation or hydrolysis of the cellulose causes an increase in the lateral sizes of the crystallites.

The two-phase model, which contains crystalline and noncrystalline domains, is currently used to describe the structural organization of cellulose [26].

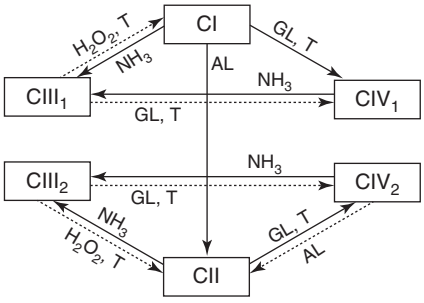

Figure 1.3 Scheme of phase transition between various crystalline allomorphs of cellulose CI (native cellulose), CII (cellulose), $CIII_1$ and $CIII_2$ (cellulose III_1 and III_2), and CIV_1 and CIV_2 (cellulose IV_1 and IV_2).

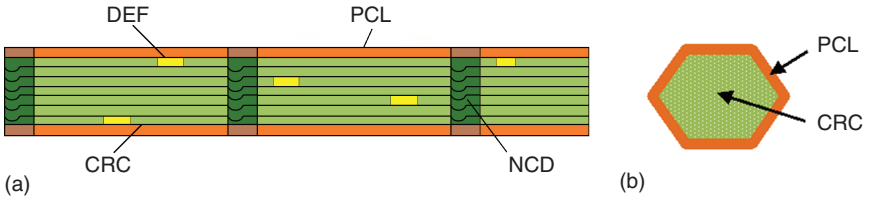

Figure 1.4 Detailed model of elementary fibril: longitudinal section (a) and cross section (b). (Ioelovich 2015 [33].)

However, further investigations have revealed the presence of a paracrystalline fraction on the crystallite surfaces that must be taken into consideration in an improved model of the cellulose structure [27]. Statistically alternated nanocrystallites, along with nanoscale noncrystalline domains, are integral constituents of long and thin elementary nanofibrils and their bundles, that is, microfibrils. The lateral sizes of elementary nanofibrils depend on the cellulose source [10, 19, 28]. This can vary over a wide range, from 3 to 4 nm for natural cellulose from herbaceous plants and woods to 10–15 nm for cellulose isolated from *Valonia algae* with lengths of several microns.

Various models of elementary fibril have been proposed in order to visualize the supermolecular structures of cellulose, such as "fringed fibrils" and "fringed micelles" [29–31]. Recently, a more detailed model of the supermolecular structure of natural cellulose has been developed [8, 27, 32]. According to this model (Figure 1.4), the elementary nanofibril of cellulose is constructed from orientated nanocrystallites and noncrystalline nanodomains (NCDs) arranged along the fibril; in addition, a thin paracrystalline layer (PCL) is located on the surface of the crystalline core (CRC). The crystallites can contain local defects (DEF), for example, vacancies, caused by the ends of the chains.

The proposed model facilitates explanation of the various physicomechanical, chemical, and biochemical properties of natural cellulose [19]. For example, it has been found that the noncrystalline domains are weak and constitute accessible points on the elementary fibrils. Therefore, processes such as acidic and enzymatic hydrolysis, alcoholysis, and acetolysis cause the cleavage of glycosidic bonds in these domains. As a result, the longitudinal splitting of the fibrils and release of crystalline particles occurs. The released nanocrystallites have the same lateral sizes as the elementary nanofibrils, but their lengths can range from 50 to 200 nm. Further details on the chemistry and structure of cellulose fibers can be found in Habibi *et al.* [34].

1.4 Main Cellulose Sources

Cellulose can be extracted from a broad range of plants, animals, and bacteria. As mentioned in the previous section, the source is very important because it affects the size and properties of the extracted cellulose. Therefore, the various sources of cellulose fiber are introduced in this section.

1.4.1 Plants

A wide variety of plant materials have been studied as regards the extraction of cellulose and NC, including wood, rice husk, sisal, hemp, flax, kenaf, and coconut husk [35]. Cotton fibers have also been used as a high-quality source material, taking advantage of their relatively low noncellulosic component content in comparison to wood [36].

Wood is an attractive starting material for cellulose and NC isolation, because of its great abundance. It is a natural composite material with a hierarchical architecture composed of cellulose, hemicelluloses, and lignin. Wood has a porous anisotropic structure, which exhibits a unique combination of high strength, stiffness, toughness, and low density [37]. The extraction of NC from wood requires a multistage process involving vigorous chemical and/or mechanical operations, which will be discussed in the following sections.

1.4.2 Tunicates

Tunicates are marine invertebrate animals, specifically, members of the subphylum Tunicata. The majority of research in this area has focused on a class of tunicates that are commonly known as *sea squirts* (*Ascidiacea*), which are a species of marine invertebrate filter feeders. Note that there are over 2300 species of *Ascidiacea* and, therefore, CMF researchers often use different species, for example, *Halocynthia roretzi* [38], *Halocynthia papillosa* [39], and *Metandroxarpa uedai* [40]. The tunicates produce cellulose in the outer tissue, termed *tunic*, from which a purified cellulose fraction termed *tunicin* can be extracted. Tunicate cellulose is composed of almost pure cellulose of CI_β allomorph type with high crystallinity. The nano-(micro- fibrils of tunicate cellulose have a very large aspect ratio (60–70) and high specific surface area (150–170 $m^2\,g^{-1}$) [41–43].

1.4.3 Algae

Algae of various species, green, red, gray, and brown, have also been considered as cellulose and NC sources. For instance, *Valonia*, *Micrasterias denticulate*, *Micrasterias rotate*, *Coldophora*, *Boerogesenia*, and other types of algae have been used [44–47]. CMFs with a large aspect ratio (>40) can be extracted from an algae cell wall through acid hydrolysis and mechanical refining [17]. The structures of CMFs isolated from different types of algae differ. For instance, *Valonia* microfibrils have square cross sections (20 nm × 20 nm) and are primarily of I_α crystalline type. Meanwhile, *M. denticulate* microfibrils have rectangular cross sections (5 nm × 20–30 nm) and are primarily of the CI_β crystalline type [46, 48, 49].

1.4.4 Bacteria

Bacterial cellulose (BC) is a product of the primary metabolic processes of certain types of bacteria. The most widely used BC-producing bacterial species is *Gluconacetobacter xylinus*. Under special culturing conditions, these bacteria produce a thick gel that is composed of CMFs and 97–99% water. BC crystallites

are primarily of the CI_{α} crystalline type and the degree of polymerization (DP) of BC is usually between 2000 and 6000. The advantage of BC is that it is possible to adjust the culturing conditions to alter the microfibril formation and crystallization. The other important feature of BC is its high chemical purity, which distinguishes it from the types of plant cellulose, which are usually associated with hemicelluloses and lignin. However, both celluloses synthesized by bacteria and cellulose extracted from various plants have similar molecular structures [7, 17, 50].

1.5 Classification of Nanocellulose Structures

The various types of NC can be classified into different subcategories based on their shape, dimension, function, and preparation method, which in turn primarily depend on the cellulosic source and processing conditions. Different terminologies have been used for the various types of NC. Recently, the Technical Association of the Pulp and Paper Industry (TAPPI) proposed standard terms and their definitions for cellulose nanomaterial WI 3021, based on the NC size [12]. The nomenclature, abbreviation, and dimensions applicable to each subgroup are shown in Figure 1.5. In this chapter, NC is categorized into six nomenclature groups using the following standard terms: microcrystal or microcrystalline cellulose (MCC), CMF, CNF, CNC, ANC, and CNY.

1.5.1 Microcrystalline Cellulose

MCC is a commercially available particulate cellulose material, which is prepared by hydrolysis of cellulose with dilute mineral acid. It consists of large multisized aggregates of nanocrystals that are bonded to each other. Commercial MCC can have spherical or rod-like particles with sizes of 10–200 μm (see, e.g., Figure 1.6a).

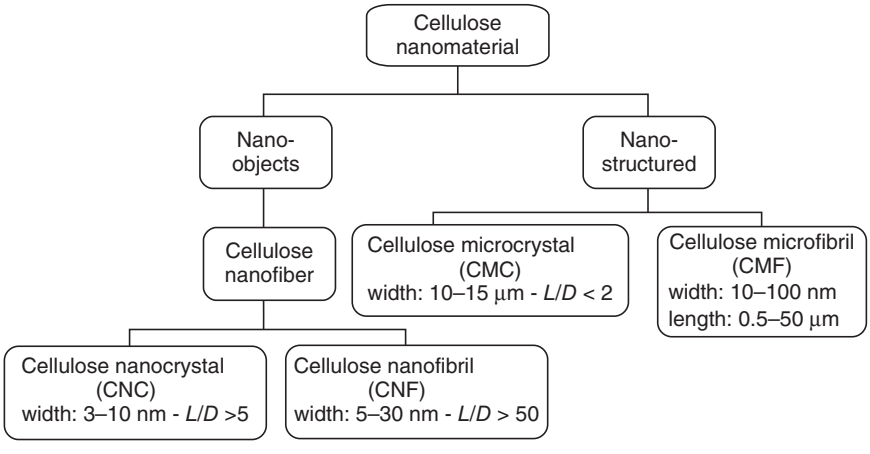

Figure 1.5 Standard terms for cellulose nanomaterials (TAPPI W13021). (Mariano *et al.* 2014 [12]. Reproduced with permission of John Wiley & Sons.)

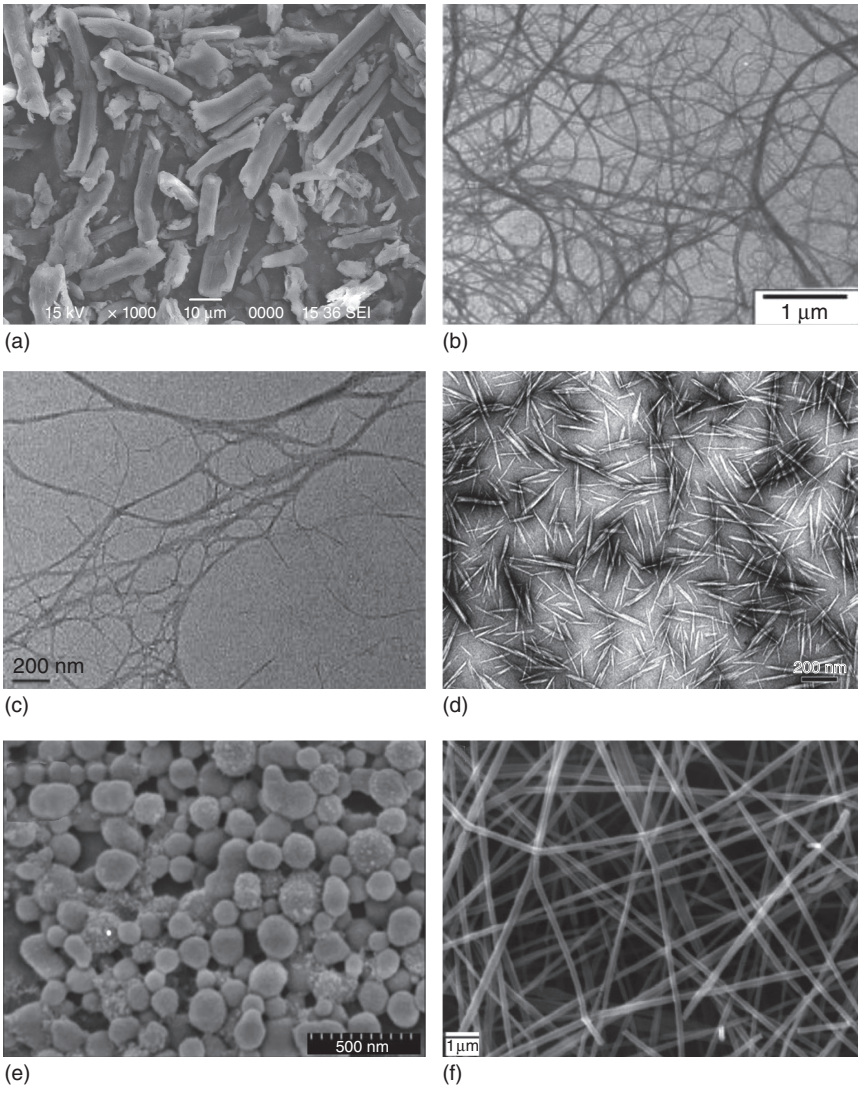

Figure 1.6 Transmission electron microscopy (TEM) micrographs of (a) MCC from fodder grass. (Adapted with Kalita *et al.* 2013 [51]. Reproduced with permission of Elsevier.) (b) CMF from sugar beet. (Dufresne *et al.* 1997 52]. Reproduced with permission of John Wiley & Sons.) (c) CNF from banana peel. (Pelissari *et al.* 2014 [53]. Reproduced with permission of Springer.) (d) CNC from ramie fiber. (Habibi *et al.* 2008 [54]. Reproduced with permission of Royal Society of Chemistry.) (e) ACN from MCC. (Loelovich 2013 [11]. Reproduced with permission of Loelovich.) (f) CNY from carboxymethyl cellulose sodium salt. (Frento *et al.* 2007 [55] Reproduced with permission of John Wiley & Sons.)

1.5.2 Cellulose Microfibrils

CMF can be produced via intensive mechanical refinement of purified cellulose pulp. CMF is considered to contain multiple aggregates of elementary nanofibrils. Microfibrils have a width of 20–100 nm and a length of 500–2000 nm (Figure 1.6b). Various other terminologies for CMF have been used in the literature, such as nanofibrillar cellulose [56], CNFs [57], or cellulose nanofibers [58].

1.5.3 Cellulose Nanofibrils

As indicated earlier, CNF and CMF terminology are sometimes used interchangeably in scientific literature, as synonyms [17]. CNFs consist of stretched bundles (aggregates) of elementary nanofibrils that are constructed from alternating crystalline and amorphous domains. CNF can be 20–50 nm in width and 500–2000 nm in length (Figure 1.6c).

CNFs are generally produced by mechanical delamination of softwood pulp in high-pressure homogenizers (HPH) without any pretreatment, or after chemical or enzymatic pretreatment [59, 60]. The resulting suspensions exhibit a clear increase in viscosity after several passes through the homogenizer. Indeed, CNFs tend to form an aqueous gel at a low concentration (typically 2 wt%), owing to the strong increase in the specific surface area in comparison to that of native cellulose fibers. Various feedstocks can be used and different treatments can be performed, which are detailed in the following sections.

A major obstacle that must be overcome for successful commercialization of CNFs is the high energy consumption required for the mechanical disintegration of the initial cellulose macrofibers into nanofibers, which often involves several passes through the disintegration device. However, preliminary 2,2,6,6-tetramethylpiperidine-1-oxyl radical (TEMPO)-mediated oxidation, carboxymethylation, mild acidic or enzymatic hydrolysis of cellulose, and certain other pretreatments significantly decrease energy consumption during the subsequent mechanical disintegration [61, 62]. To date, it seems that the type of cellulose feedstock used plays a significant role in the energy consumption; however, it has only a minor influence on the final CNF properties [63].

It must be noted that CNFs have certain negative properties, which limit their usage in several applications, for example, in papermaking because of slow dewatering or as polymer composites owing to poor compatibility of hydrophilic reinforcers with hydrophobic polymers [63]. The most feasible solution to this problem is the chemical modification of CNFs in order to reduce the number of hydrophilic hydroxyl groups, which is described in Chapter 3.

1.5.4 Cellulose Nanocrystals

CNC exhibits an elongated rod-like shape and has very limited flexibility compared to CNF, because of its higher crystallinity [59]. CNCs are also known as nanocrystalline cellulose, nanowhiskers, nanorods, and rod-like cellulose crystals (Figure 1.6d).

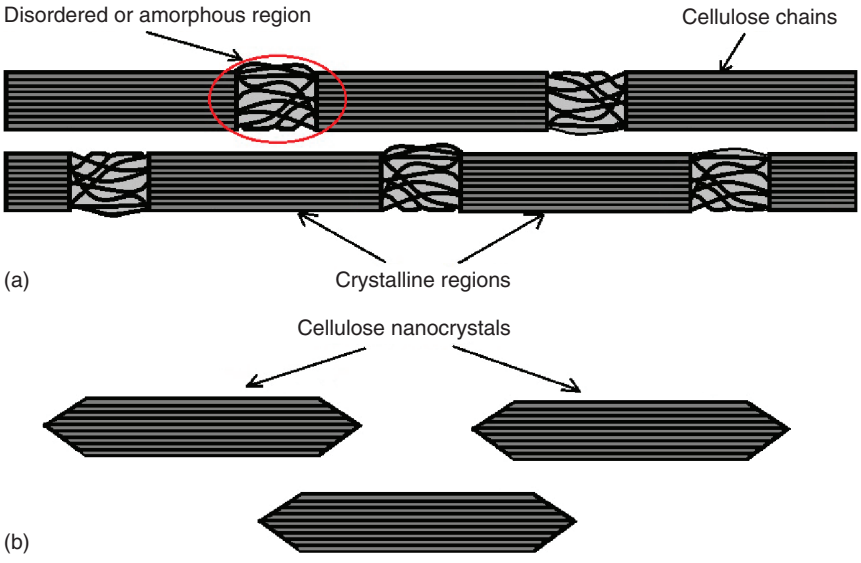

Figure 1.7 (a) Suggested arrangement of crystalline and amorphous domains in cellulose nanofibrils and (b) isolated cellulose nanocrystals. (Moon *et al.* 2011 [17]. Reproduced with permission from Royal Society of Chemistry.)

The nanocrystalline particles are generated by the splitting of amorphous domains, as well as by the breaking of local crystalline contacts between nanofibrils, through hydrolysis with highly concentrated acids (6–8 M). This chemical process is followed by high-power mechanical or ultrasonic treatments (Figure 1.7). An important characteristic of CNCs prepared using sulfuric acid (SA) is the negative particle charge due to the formation of sulfate ester groups, which enhances the phase stability of the nanocrystalline particles in an aqueous medium.

The geometrical dimensions of CNCs can vary widely, with diameter in the range of 5–50 nm and length in the range of 100–500 nm. The dimensions and crystallinity of a given CNC depend on the cellulose source and extraction conditions [34, 64]. It has been reported that nanocrystalline particles extracted from tunicates and BC are usually larger compared to CNCs obtained from wood or cotton. This is because tunicates and BC are highly crystalline and contain longer nanocrystallites [41]. CNCs extracted from pure cellulose materials exhibit increased crystallinity [17].

Nanocrystalline cellulose particles exhibit excellent mechanical properties. The theoretical Young's modulus of a CNC along the cellulose chain axis is estimated to be 167.5 GPa, which is similar to the modulus of Kevlar and even higher than the modulus of steel [65]. The experimental Young's modulus of cotton CNCs is 105 GPa and the modulus of tunicate CNCs is 143 GPa [42, 66]. Similar to other types of NC, CNCs can also be successfully functionalized in order to reduce hydrophilicity and to facilitate the incorporation of the modified nanoparticles into a hydrophobic polymer matrix [34].

1.5.5 Amorphous Nanocellulose

ANC can be obtained through acid hydrolysis of regenerated cellulose with subsequent ultrasound disintegration [11, 19, 61]. ANC particles usually have an elliptical shape with average diameters of 50–200 nm (Figure 1.6e). Because of its amorphous structure, ANC exhibits specific features, such as increased functional group content, high accessibility, enhanced sorption, and enhanced thickening ability. However, ANC particles have poor mechanical properties and are unsuitable for use as reinforcing nanofillers. Therefore, the primary applications of ANC are as carriers for bioactive substances, thickening agents in various aqueous systems, and so on.

1.5.6 Cellulose Nanoyarn

CNY has not been widely studied to date. It is manufactured by electrospinning a solution composed of cellulose or cellulose derivatives [67–69]. A transmission electron microscope (TEM) image of nanoyarn produced from carboxymethyl cellulose sodium salt is shown as an example in Figure 1.6f. The majority of the obtained electrospun nanofibers have diameters ranging from 500 to 800 nm, and X-ray investigations have shown that regenerated nanoyarn has low crystallinity and is a CII allomorph. In addition, the thermal stability of the electrospun nanofibers is significantly lower than that of the initial cellulose material. The DP of CNY is most likely close to the DP of conventional hydrate cellulose fibers, that is, 300–600. The CNY preparation technique is detailed in the following sections.

1.6 Preparation Techniques of Various Types of Nanocellulose

1.6.1 Preparation of CNF/CMF

If plant cell wall is subjected to strong mechanical disintegration, the original structure of cellulose fiber is degraded and the fibers turn to nanofibrils (CNF) or their microfibril bundles (CMF) with diameters in the range of 10–100 nm depending on the disintegration power. The length of the obtained fibrils can extend to some microns. Several mechanical techniques can be used to extract CNF or CMF from various feedstocks, namely, homogenization, microfludization, grinding, cryocrushing, and ultrasonication, as discussed below.

1.6.1.1 High-Pressure Homogenization

HPH is a widely used method for large-scale production of CNF, as well as for laboratory-scale preparation of nanofibrils. This technique involves forcing the suspension through a very narrow channel or orifice using a piston, under a high pressure of 50–2000 MPa (Figure 1.8). The width of the homogenization gap depends on the viscosity of the suspension and the applied pressure, and ranges from 5 to 20 μm.

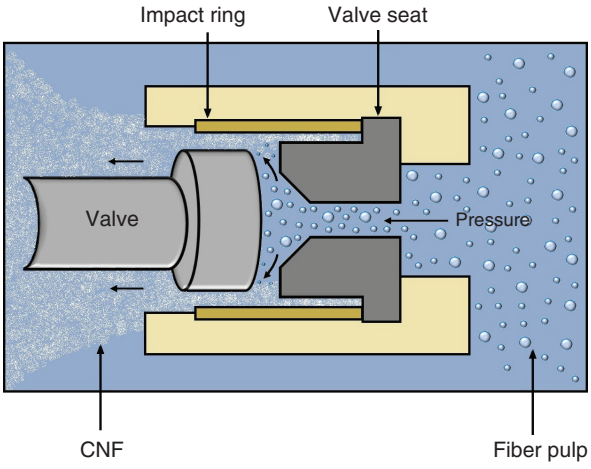

Figure 1.8 Schematic of homogenizer.

The resultant high suspension streaming velocity causes an increase in the dynamic pressure and a reduction in the static pressure below the vapor pressure of the aqueous phase. This leads to the formation of gas bubbles that collapse immediately when the liquid leaves the homogenization gap, being again under a normal air pressure of 100 kPa. The gas bubble formation and implosion phenomenon induces the formation of shockwaves and cavitations, which cause disruption of the fibrillar structure of the cellulose [70].

Cellulose fiber size reduction can be achieved through a large pressure drop, high shear forces, turbulent flow, and interparticle collisions. The extent of the cellulose fibrillation depends on the number of homogenization cycles and on the applied pressure. The higher the pressure, the higher the efficiency of the disruption per pass through the machine [71].

Various cellulosic materials have been subjected to homogenization, such as wood pulp [72], cotton [73, 74], *Helicteres isora* plant fiber [75], mangosteen rind [76], and sugar beet [77]. For example, to extract CNF from bleached cellulose residues, Habibi *et al*. [78] performed 15 homogenization passes at 50 MPa at temperatures below 95 °C.

However, some problems appear during the manufacturing of nanofibrillated cellulose from pulp, which are caused by the following:

1) Insufficient disintegration of the pulp fibers and clogging of the homogenizer when the pulp is pumped through a very small orifice. To overcome this problem, various mechanical pretreatments are used before homogenization, such as grinding, milling, refining, cryocrushing, or ultrasonication [79–83].
2) High energy consumption. To overcome this problem, the pulp can be subjected to prior chemical purification or pretreatment using acid hydrolysis, oxidation, enzymatic hydrolysis, and certain other pretreatment techniques.
3) Excessive mechanical damage of the crystalline structure of the CNF [84].

1.6.1.2 Microfluidization

A microfluidizer is another tool that can be used for CNF or CMF preparation. Unlike the homogenizer, which operates at constant pressure, the microfluidizer

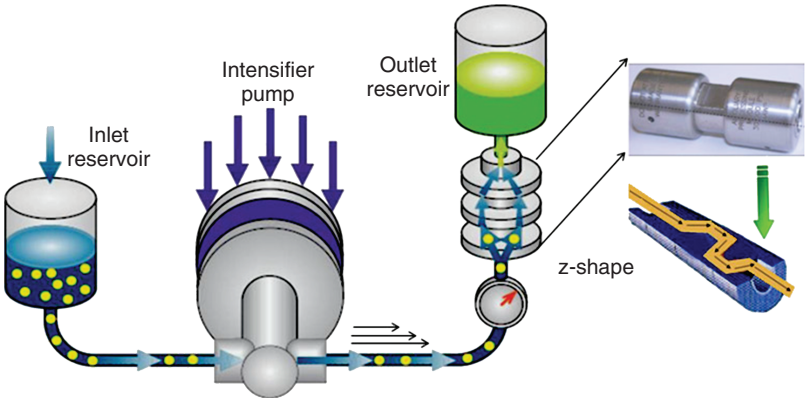

Figure 1.9 Microfluidizer schematic. (Missoum *et al.* 2013 [63].)

operates at a constant shear rate. The fluid slurry is pumped through a z-shaped chamber, where it reaches a high shear force (Figure 1.9).

The pressure can reach levels as high as 40 000 psi, that is, approximately 276 MPa. Specially designed fixed-geometry microchannels are positioned within the chamber, through which the pulp slurry accelerates to high velocities. The desired shear and impact forces are created when the slurry stream impinges on wear-resistant surfaces. A series of check valves allow recirculation of the slurry. Upon exiting the interaction chamber, the product may be directed through a heat exchanger, recirculated through the system for further processing, or directed externally to the next step in the process. It is necessary to repeat the process several times and to use differently sized chambers in order to improve the degree of fibrillation [7, 63, 64, 71, 85].

Lee *et al*. [86] examined the effect of the number of passes of MCC slurry through a microfluidizer on the morphology of the obtained CNFs. They found that the aspect ratio of the nanofibrillar bundles increased after 10–15 passing cycles, whereas an additional 20 passes led to agglomeration of the CNFs due to increased surface area and higher surface hydroxyl group content.

Three different types of empty palm fruit bunch fiber (EPFBF) cellulose pulp were subjected to refining and microfluidization processes to obtain CNF [87]. Morphological characterization of the results demonstrated that microfluidization could generate nanofibers with a more homogeneous size distribution. It was found that microfluidization did not change the kappa number of the CNF significantly, compared to the original pulp. Furthermore, the CNF from EPFBF had superior properties to that obtained from bleached fibers.

1.6.1.3 Grinding

Another technique for separating cellulose fibers into nanosized fibrils is grinding. During grinding, a fiber fibrillation process is conducted by passing the cellulose slurry between static and rotating grindstones revolving at approximately 1500 rpm, which applies a shearing stress to the fibers (see Figure 1.10). The fibrillation mechanism in the grinder utilizes shear forces to degrade the cell

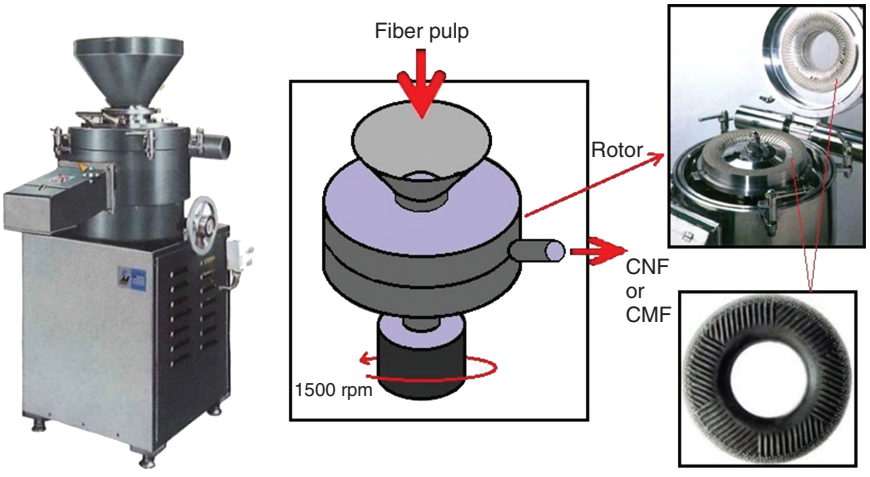

Figure 1.10 Grinder system. (Missoum 2013 [63].)

wall structure and individualize the nanoscale fibrils [62]. The extent of fibrillation is dependent on the distance between the disks, the morphology of the disk channels, and the number of passes through the grinder. As for a homogenizer, many passes are required to generate the fibrillated cellulose. The need for disk stone maintenance and replacement can be a disadvantage of this technique, as wood pulp fibers can erode the grooves and grit. However, a primary advantage of grinder processing is that additional mechanical pretreatments are not required [71].

Wang *et al*. [88] investigated the effect of energy consumption and fibrillation time on crystallinity and the DP of a 2% pulp suspension. They found that the energy input increased from 5 to 30 Wh kg^{-1} after 11 h of grinding, leading to a noticeable decrease in the DP and crystallinity index of the cellulose. Furthermore, the heat produced by friction during the fibrillation process led to water evaporation, increasing the pulp consistency from 2% to 3.2%. As a result of the grinding, two main structures were disclosed: first, untwisted fibrils, and second, twisted and entangled nanofibers.

Hassan *et al*. [89] produced nanofibers by passing bleached pulp made from rice straw and bagasse through a high-shear grinder and an HPH, using 30 and 10 passes, respectively. They found that treatment with the homogenizer led to nanofibers of smaller and more uniform size. On the other hand, it was not possible to complete the fibrillation process using a high shear grinder only. One of the important parameters that affects the characteristics of the obtained CNFs is the number of passes through the grinder or HPH. Iwamoto *et al*. [90] reported that 14 passes were required for sufficiently fibrillated pulp to be produced in their study, while extra cycles of up to 30 passes for the pulp fiber did not promote further fibrillation. After 10 grinding repetitions, nanofibers with uniform widths of 50–100 nm were obtained. In addition, Iwamoto *et al*. [91] studied the fibrillation of dissolved pulp after 1–30 passes at 1500 rpm. Bundles of nanofibrillated pulp that have a width of 20–50 nm were produced after five passes through the grinder, and further passes did not change the dimensions

of the NFC. They also reported that the DP and crystallinity decreased with an increased number of passes.

1.6.1.4 Cryocrushing

Cryocrushing is a mechanical fibrillation method for cellulose in a frozen state [92, 93]. This method produces fibrils with relatively large diameters, ranging between 0.1 and 1 μm [93]. In this process, water-swollen cellulose fibers are frozen in liquid nitrogen and subsequently crushed [94]. The application of high impact forces to the frozen cellulosic fibers leads to rupturing of the cell walls due to the pressure exerted by the ice crystals. This liberates the nanofibers [62]. The cryocrushed fibers may then be dispersed uniformly in water using a routine disintegrator. This procedure is applicable to various cellulose materials and can be used as a fiber pretreatment process before homogenization. Wang and Sain [95, 96] produced nanofibers from soybean stock through cryocrushing and subsequent high-pressure fibrillation. TEM showed that the nanofiber diameters were in the 50–100 nm range. The nanofibers prepared exhibited superior dispersion ability in acrylic emulsion compared to water. However, the cryocrushing method has low productivity and is expensive, because of its high energy consumption.

1.6.1.5 High-Intensity Ultrasonication

High-intensity ultrasonication (HIUS) is a common laboratory mechanical treatment used for cell disruption in an aqueous medium. This treatment generates efficient cavitations that include the formation, expansion, and implosion of microscopic gas bubbles, when the water molecules absorb ultrasonic energy. The action of the hydrodynamic forces of the ultrasound on the pulp leads to the defibrillation of the cellulose fibers [97].

Many researchers have studied the application of HIUS to the isolation of nanofibers from various cellulosic sources, such as pure cellulose, MCC, pulp, culinary banana peel, rice waste, and microfibrillated cellulose [98–103]. The results show that a mixture of microscale and nanoscale fibrils can be obtained following ultrasonication of the cellulose samples; the diameters of the obtained fibrils are widely distributed from 20 nm to several microns, indicating that some nanofibrils are peeled from the fibers, whereas some remain on the fiber surface [104, 105]. Thus, this method gives aggregated fibrils with a broad width distribution. It has been also found that the crystalline structure of some cellulose fibers is altered through ultrasonic treatment. These changes differ for different cellulose sources, for example, the crystallinity after treatment increased for pure cellulose, decreased for MCC, while it remained constant for pulp fiber.

Wang and Cheng [105] evaluated the effects of temperature, concentration, power, size, time, and distance from the probe tip on the degree of fibrillation of some cellulose fibers using HIUS treatment. They reported that superior fibrillation was caused by higher power and temperature, while longer fibers were less defibrillated. Higher pulp concentration and larger distance from the probe to beaker were not advantageous for the fibrillation. These researchers found that a combination of HIUS and HPH improves the fibrillation and uniformity of the nanofibers, compared to HIUS alone. The NFC yield can be also increased,

when TEMPO-oxidized pulp is used for HIUS treatment [106]. The combination of blending and HIUS treatments was found to be more efficient for the production of NC in contrast to HIUS alone. Chen *et al*. [107] showed that the temperature can reach a specific degradation point when a prolonged HIUS treatment with 1 kW power at 20.25 kHz is used. All ultrasound methods involve high energy consumption and can cause a dramatic decrease in the NFC yield and fibril length.

1.6.2 CNC Preparation

The isolation of CNCs from plant sources is generally conducted in three steps. The first step is purification of the raw material to remove noncellulose components from the plant material and to isolate purified cellulose. The purification can be performed, for example, with sodium or potassium hydroxide, followed by bleaching with sodium chlorite, as reported in Section 1.7. This procedure can be repeated several times for more effective purification of the cellulose. The second step is a controlled chemical treatment, generally acid hydrolysis, which is used to split the amorphous domains, remove local interfibril crystalline contacts, and release CNCs after the third step – the subsequent mechanical or ultrasound treatment (refer to Figure 1.7).

1.6.2.1 Acid Hydrolysis

To release CNCs, acid hydrolysis of purified cellulosic material is conducted using strong mineral acids (6–8 M) under controlled temperature, time, agitation, and acid/cellulose ratio conditions. Different mineral acids can be used for this purpose, such as sulfuric [34], hydrochloric [108, 109], phosphoric [110–112], maleic [113], hydrobromic [110–112], nitric [114], and formic acids [115]. A mixture composed of hydrochloric and organic acids (acetic or butyric) has also been reported [116].

SA is the most extensively used acid for CNC preparation. During hydrolysis, disordered amorphous domains and local interfibrillar contacts of cellulose are preferentially hydrolyzed, whereas stable crystallites remain intact and can be isolated as rod-like nanocrystalline particles [117]. The CNC dispersion in a strong acid is diluted with water and washed using successive centrifugations. Neutralization or dialysis with distilled water is performed to remove free acid from the dispersion. Additional steps such as filtration [38], centrifugation [118], or ultracentrifugation [119], as well as mechanical or ultrasound disintegration, have also been reported.

If CNCs are prepared using cellulose hydrolysis with hydrochloric acid (HA), the uncharged nanocrystalline particles tend to flocculate in aqueous dispersions [108]. On the other hand, when SA is used as a hydrolyzing agent, it reacts with the surface hydroxyl groups of nanocrystallites leading to the formation of negatively charged sulfonic groups (Figure 1.11). The acid hydrolysis of cellulose chains in amorphous domains involves rapid protonation of glucosidic oxygen (path 1) or cyclic oxygen (path 2), followed by a slow splitting of the glucosidic bonds induced by the addition of water (Figure 1.11a). This hydrolysis process yields two shorter chain fragments, while preserving the basic backbone structure.

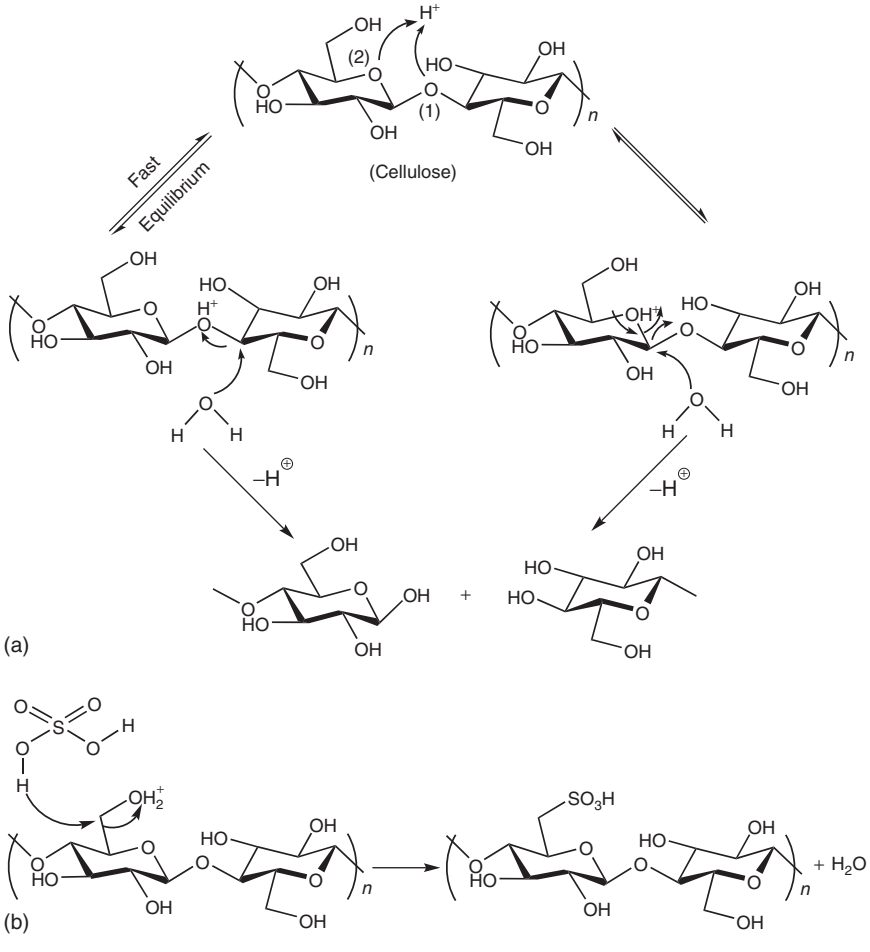

Figure 1.11 (a) Mechanism of cellulose chain acid hydrolysis and (b) esterification of cellulose nanocrystals. (Adapted with Lu and Hsieh 2010 [120]. Reproduced with permission of Elsevier.)

Besides chain scission, the hydrolysis of cellulose with SA also involves partial esterification of the hydroxyl groups (Figure 1.11b). The presence of sulfate groups results in the negatively charged surface of nanocrystals. This anionic stabilization via the repulsion forces of electrical double layers is very efficient in preventing the aggregation of CNCs [120]. However, the introduction of acidic sulfate groups compromises the thermostability of the NC [121]. To increase the thermal stability of the nanocrystals, neutralization of sulfate groups to pH > 7 using sodium hydroxide has been proposed [122].

The effect of hydrolysis conditions on the morphology, yield, and properties of CNC has been studied in [122–125]. Typically, higher acid concentrations, longer reaction times, and higher temperatures lead to higher surface charge and narrow sizes, but to lower yield and decreased crystallinity and thermal stability of CNC. For example, after cellulose hydrolysis with 63.5 wt% SA, the yield of CNC was

approximately 30%, whereas after hydrolysis with 65 wt% SA the yield of CNC was decreased to ≤20%. When the SA concentration was reduced to 60 wt%, the CNC yield increased to its maximum value, 65–70% [61, 126].

As an example, consider the CNC preparation method using the hydrolysis of cotton cellulose with aqueous solutions of SA given by Ioelovich [61]. Here, the acid concentration was 50–70 wt% with an acid/cellulose ratio of 8–10. The reaction was conducted at 45 °C for 40–60 min, and the final dispersion of washed CNCs in water was obtained via sonication using an ultrasound disperser at 20 kHz for 10–15 min. According to the results of X-ray investigations, in the acid concentration range of 50–60 wt% the crystallinity of the obtained CNCs increased slightly. On the other hand, when the acid concentration was higher than 60 wt%, partial decrystallization of the nanoparticles occurred, because of increased solubility in the sufficiently concentrated SA medium.

Characterization of the output showed that cellulose hydrolysis with 60 wt% acid gave a CNC yield of 65–70 wt%. When the acid concentration was above 65 wt%, the cellulose sample was completely dissolved. The yield of particles composed of cellulose and regenerated from 65 wt% acid was low (about 20 wt%). Furthermore, these particles exhibited a decreased degree of crystallinity (about 30%) and DP (about 60). Increasing the acid concentration to over 65 wt% led to further diminution in the yield, crystallinity, and DP of the regenerated particles. After hydrolysis of the initial sample with 67 wt% acid, the particle yield was zero, because hydrolyzed and dissolved cellulose cannot be regenerated from an acidic solution by dilution with water. In this case, this was because of the fast acidic depolymerization of the cellulose with the 67 wt% acid, along with the formation of water-soluble oligomers.

Electron microscopic observation showed that after cellulose hydrolysis with 50–55 wt% SA CNC aggregates with 300–500 nm length and 40–60 nm lateral size were formed. An increase in the acid concentration to approximately 60 wt% contributed to the formation of smaller CNCs with sizes of 100–200 nm × 10–20 nm. Thus, the reduced acid concentration of 50–55 wt% led to the formation of overly coarse aggregates, while higher concentrations (>60 wt%) led to a low nanoparticle yield with decrystallized structures. To obtain small and highly crystalline nanoparticles at maximum yield, the concentration of SA used for hydrolysis of the starting cellulose material should be approximately 60 wt% [61]. Compared to the hydrolysis procedure using SA, cellulose hydrolysis with HA requires a higher temperature (60–80 °C) in order to produce CNCs of similar dimensions [127, 128].

Recently, Guo *et al*. [129] reported that ultrasonication treatment while hydrolysis reaction promotes an increase in CNC yields when short hydrolysis times (45 min) are involved. In addition, ultrasonic treatment led to CNCs having shorter lengths and narrower size distributions. However, a further acid hydrolysis during ultrasonic treatment caused the widths and thickness of CNCs to decrease, owing to delamination and disorder in the cellulose crystalline structure generated by a partial dissociation of cellulose hydrogen bond networks in the CNCs while undergoing ultrasonic treatment with long hydrolysis periods. The characteristics of CNCs prepared from different cellulose sources are given in Table 1.1.

Table 1.1 Hydrolysis conditions for the preparation of nanocrystals from different cellulosic fibers and sizes, aspect ratios (*L/D*), and crystallinity index (CI) of isolated CNCs.

Source	Acid (wt%)	*T* (°C)	Time (min)	Acid/cellulose ratio	Diameter (nm)	Length (nm)	*L/D*	CrI (%)	References
Sisal	H_2SO_4, 32%	45	45	14 : 0.6 v/v	10 ± 5	403 ± 159	40	78	[130]
Maize stalk residue	H_2SO_4, 50%	40	30	20 : 1 v/w	3–7	150–450	50–64	72.6	[2]
Coconut husk	H_2SO_4, 30 v/v%	60	6 h	8.75 : 1 v/w	8 ± 3	172 ± 88	22 ± 8	82	[131]
Potato peel	H_2SO_4, 64%	45	90	17.5 : 1 v/w	?	140	41	85	[132]
Switch grass	H_2SO_4, 60%	45	45	15 : 1 v/w	3.9 ± 1.3	148.1	38	69	[133]
Corncob	H_2SO_4, 9.7 M	45	60	15/1 v/w	4.15 ± 1.08	210.8 ± 44.2	53.4 ± 15	83	[134]
Sugarcane bagasse	H_2SO_4, 64%	45	60	10 : 1 v/w	20–60	250–480	8–12.5	72.5	[135]
BC	H_2SO_4 37%	60	48 h	—	1103 ± 698	14 ± 7.4	94 ± 79	72	[136]
Tunicate	H_2SO_4, 48%	60	20	20 : 1 w/w	1187 ± 1066	9.4 ± 5	148 ± 147	80	
Wood pulp	H_2SO_4, 64%	—	—	—	130 ± 67	5.9 ± 1.8	23 ± 12	60	
Soy hulls	H_2SO_4, 64%	40	30	30 : 1 v/w	2.77 ± 0.67	122.66 ± 9.4	44	73	[3]
Rice straw	H_2SO_4, 64%	45	45	8.75 : 1 v/w	11.2	117	10.5	91.2	[137]
Kenaf	H_2SO_4, 65%	45	40	20 : 1 w/w	12 ± 3.4	158.4 + 63.6	13.2	81	[122]
Mangkpuan	H_2SO_4, 60%	45	45	20 : 1 w/w	5–25	50–400	10–20	—	[138]
Agave	H_2SO_4, 60%	45	45	20 : 1 w/w	8–15	170–500	10–45	82	[139]
Cotton linter	H_2SO_4, 60%	45	90	20 : 1 w/w	15–50	210–480	—	87–89	[140]
Oil plam trunk	H_2SO_4, 64%	45	60	—	4–10	176–892	—	57–63	[141]
Tomato peels	H_2SO_4, 64%	45	30	—	1–7	100–200	—	80.8	[142]
Waste paper	H_2SO_4, 60 v/v%	45	60	20 : 1 w/w	3–10	100–300	—	75.9	[143]
Onion skin	H_2SO_4, 45%	60	3 h	20 : 1v/w	35 ± 7	356 ± 85	10.1	26	[144]
Macrophyte typha domingensis	H_2SO_4, 34%	80	15	—	12.6 ± 4.4	593 ± 482	47	74	[145]
Beer industrial residues	HCl, 10%	80	2, 4, and 6 h	—	73–146	—	—	79–89	[146]
Bamboo	HNO_3, 30%	50	1440	—	50–100	—	—	46.08	[114]
	HPO_3, -	40–60	1.5–3.5 h	30 : 1 w/w	15–30	100–200	—	59	[147]
MCC	HBr, 1.5–2.5 M	100	240	—	—	—	—	35	[148]
Lyocell fibers	HCOOH/HCl, 6 M (9 : 1)	70–90	6–12 h	—	19–29	—	—	—	[115]

Under similar hydrolysis conditions, the crystallinity and dimensions of the nanocrystalline particles depend on the origin of the cellulose feedstock [19, 34, 128]. For example, after acid hydrolysis, tunicate samples yield highly crystalline and long nanoparticles with a high aspect ratio, while wood cellulose yields less crystalline and shorter nanoparticles with a lower aspect ratio. Generally, nanocrystalline particles isolated from the cellulose of various terrestrial plants have lateral sizes ranging from 4 to 20 nm and lengths of 100–300 nm, whereas the nanoparticles isolated from non-terrestrial sources, such as tunicate, algae, and BC, are longer and thicker [19, 34, 36, 41, 128].

1.6.2.2 Hydrolysis with Solid Acids

Although acid hydrolysis is widely used for the production of CNCs, certain problems must be overcome, such as high consumption of energy and chemicals, acidic corrosion of equipment, and health and environmental hazards. Recently, a number of studies have focused on hydrolysis parameter optimization, corrosion prevention, and waste reduction [149]. An interesting proposal has been made, in which it was suggested that the strong liquid acid used in this process should be replaced by a solid acid. For example, a hydrolysis procedure using an acidic cation exchange resin as a solid catalyst in combination with high-power disintegration has been reported to produce cellulose particles with a yield of approximately 50%, and the solid acid can be regenerated using a post-treatment procedure [150]. Recently, Liu *et al*. [149] reported preparation of cellulose nanoparticles with diameters of 15–40 nm and lengths of hundreds of nanometers using the hydrolysis of bleached pulp with solid phosphor-tungsten acid ($H_3PW_{12}O_{40}$). They found that the resultant CNCs exhibited a significantly higher thermal stability than the CNCs prepared using hydrolysis with SA. In addition, the solid acid could be easily recovered and recycled through extraction with diethyl ether.

The major advantages of hydrolysis with a solid acid are easy recovery of the solid acid, low equipment corrosion, and a relatively safe working environment. Moreover, the recovered acid can be reused several times for further cellulose hydrolysis without loss of acid activity or reduction of the final product yield. The primary shortcomings of this hydrolysis method are the very high cost of solid acid, as well as prolonged hydrolysis time, low productivity, the heterogeneity of the hydrolysis process, and wide particle size distribution, which are caused by limited contact between the solid acid granules and the cellulose feedstock. However, Hamid *et al*. [151] reported that sonication in combination with solid phosphor-tungsten acid reduces dramatically the time of operation from 30 h to 10 min by using an optimum sonication power of 225 W. The size of the obtained CNCs was in the range from 15 to 35 nm in diameter and 150 to 300 nm in length with crystallinity of about 88% and yield of 85%.

1.6.2.3 Hydrolysis with Gaseous Acids

In this technique, wet cellulose with a moisture content of up to 80% is hydrolyzed in the presence of an acidic gas. The gaseous acid is absorbed by the cellulose fibers and reacts with the moisture of the material; as a result, a high local acid concentration is obtained. This leads to a high rate of hydrolysis

of the amorphous domains and of the local interfibril contacts. Then, CNCs are isolated using mechanical grinding and/or ultrasound treatment of the hydrolyzed cellulose. Various types of gaseous acids can be used in this procedure, such as HA, nitric acid, and trifluoroacetic acid. This technique can allow several environmentally harmful and time-consuming steps that are required for classical acid hydrolysis to be omitted. Indeed, large amounts of water are not necessary, the acid recycling is easier, and the dialysis step can be omitted. The CNC yield is also higher, because of lower cellulose feedstock loss during the gaseous hydrolysis process [152].

1.6.2.4 Hydrolysis with Metal Salt Catalyst

Metal inorganic salts in the trivalent ($FeCl_3$, $Fe_2(SO_4)_3$, $Al(NO_3)_3$), divalent ($CaCl_2$, $FeCl_2$, $FeSO_4$), and monovalent (NaCl, KCl) categories have been demonstrated by many researchers for enhancing the hydrolysis efficiency of cellulose [153–156] and preparation of micro- or nanocrystalline cellulose [157–159]. A transition metal-based catalyst provides a feasible, selective, and controllable hydrolysis process with mild acidity. In fact, the valence state of the metal ion is the key factor to influence the hydrolysis efficiency, where an acidic solution (H^+) generates during polarization between metal ions and water molecules. A higher valence state generates more H^+ ions, which act effectively in the co-catalyzed acid hydrolysis reaction in the presence of metal ions [154, 160].

Lu *et al*. [158] have reported the use of $FeCl_3$ for the hydrolysis of cellulose into NC. It was indicated that the reagent diffuses into the amorphous regions of cellulose and promotes the cleavage of glycosidic linkages of cellulose chains into smaller dimensions. Furthermore, the presence of an acidic medium (HCl) or ultrasonic-assisted treatment can act synergistically to improve the accessibility of metal ions for the hydrolysis process [157, 158, 161].

Recently, Hamid *et al*. [160] proposed the nickel-based inorganic salt (nickel(II) nitrate hexahydrate) for the selective transformation of MCC into NC. It was revealed that the NC produced via 40% H_2SO_4 hydrolysis has lower aspect ratio compared with nickel-catalyzed NC. Acid hydrolysis NC rendered shorter length of nanocrystals while nickel-catalyzed NC showed fine width with controllable length of products. This indicated that Ni-based inorganic salt is capable of selectively controlling the hydrolysis as compared to SA reaction.

1.6.2.5 Other Preparation Techniques

Other CNC preparation techniques include treatment with ionic liquid (IL), enzymatic hydrolysis, and TEMPO-mediated oxidation. However, these techniques are usually applied in combination with other chemical and mechanical or ultrasound treatments.

ILs have recently been used as both solubilizing agents and catalysts for cellulose hydrolysis. For example, the treatment of MCC with 1-butyl-3-methylimidazolium hydrogen sulfate ($BmimHSO_4$), with the possible reuse of the IL, has been described [162]. However, the obtained CNCs exhibited a low thermal stability in this case. Advanced reaction media such as "deep eutectic solvents" have recently been generated and appear to be potentially useful ionic

solvents. They can be prepared simply through the mixing of hydrogen bond donors with halide salts [163, 164]. The usefulness of advanced IL for CNC extraction is related to a simple and effective hydrolysis process in the homogeneous IL medium [165].

The literature on the use of enzymatic hydrolysis for the extraction of NC focuses primarily on CNF or CMF preparation. One exception is a quite detailed paper by Siqueira *et al*. [166], in which various combinations of enzymatic hydrolysis and mechanical shearing to produce nanoparticles from sisal pulp are investigated. These researchers report that, depending on the treatment conditions and their sequence, CNCs can coexist with microfibrils in the obtained suspensions. Filson *et al*. [167] prepared CNCs from recycled pulp using hydrolysis with endoglucanase enzyme in a microwave; they observed that microwave heating permits faster nanoparticle production with higher yield compared to conventional heating. This is because microwave heating is more selective.

The TEMPO-meditated oxidation method has also been applied to cellulose fibers to produce CNCs. It has been reported that isolated CNCs reveal superior dispersity in water after TEMPO oxidation, because of the incorporation of a higher number of carboxylate groups in the cellulose. In addition, the oxidized nanoparticles exhibit smaller sizes, improved transmittance, higher shear stress, and higher viscosity compared to CNCs obtained using the conventional hydrolysis method [168]. Further details of TEMPO-meditated oxidation are given in Section 1.7.

Recently, solvothermal pretreatment of cellulose with ethanol and peroxide followed by ultrasonic treatment has been used to produce CNCs [169]. Organosolv treatment is an important pretreatment method for biomass refinery. It results in an efficient fractionation of lignocellulose into its main components, thus allowing the valuable conversion into useful products. In this method, various organic solvents such as alcohols, esters, ketones, phenols, and amines act as dissolving agents by solubilizing lignin and some of hemicellulose under heating conditions and leaving relatively pure cellulose. Solvents with low boiling point (e.g., ethanol) are the major solvents that are usually used because of their low cost, solubility in water, and ease of recovery. Li *et al*. [169] reported that solvothermal treatment with ethanol can fractionate 97% of total lignin and 70% of the hemicellulose, and the subsequent treatment with peroxide can remove the rest of the lignin and one-third of the remnant hemicelluloses and produce 95% of pure cellulose. The resultant CNCs isolated after ultrasonic processing were 1–9 nm wide and 500 nm long, with aspect ratios ranging from 10 to 150. Higher crystallinity and thermal stability of produced CNCs has also been reported compared with CNCs prepared by traditional methods.

1.6.3 Preparation of Nanoparticles of Amorphous Cellulose

The main method used for ANC production is the acid hydrolysis of low-crystalline cellulose feedstock. For this purpose, an initial cellulose material should be preliminarily dissolved in 66–67% SA, in 85% phosphoric acid (PA), in a mixture of concentrated SA and PA, or of concentrated SA

and HA at room or lower temperature (preferably at 10–15 °C). When the acidic condition is maintained for 40–60 min, depolymerization of the cellulose macromolecules occurs. After regeneration of the hydrolyzed cellulose from the solutions, amorphous flocks of low-molecular-weight cellulose are formed. Disintegration with an ultrasound disperser contributes to conversion of the flocks into amorphous nanoparticles [11, 19, 170]. The obtained particles have spherical to elliptical shapes with diameters ranging from 80 to 120 nm, depending on the cellulose origin, extraction method, and isolation conditions. It has been discovered that the diameter of the particles can be reduced to 50–80 nm after prolonged sonication [171].

An example of fabrication of ANC nanoparticles using the hydrolysis of cotton cellulose with 66 wt% SA has been described in papers by Ioelovich [11, 19]. The produced nanoparticles have a DP of 60–70 and a maximum yield of 65–70%. Increasing the acid concentration to over 66 wt% leads to a decrease in the yield of ANC. After hydrolysis with 70–72 wt% SA, the dissolved cellulose cannot be regenerated from the acidic solution through dilution with water, because of the rapid acidic depolymerization of the cellulose and the formation of water-soluble oligomers. Because of their amorphous structure, the nanoparticles acquire specific features such as increased negatively charged functional group content, high accessibility, and high sorption ability. Freeze-dried ANC absorbs up to 35–40% water vapor and decomposes completely under the action of cellulolytic enzymes. However, the thermal stability and mechanical properties of ANC nanoparticles are poor; therefore, these nanoparticles are not suitable for use as reinforcing nanofillers.

Preparation method of spherical ANC nanoparticles using hydrolysis with the mixture of SA and HA in combination with prolonged sonication has been reported by Wang *et al*. [172, 173]. These researchers have recognized that nanoparticles cannot be obtained in the absence of ultrasonic treatment. Spherical amorphous nanoparticles can also be prepared following special pretreatment of the initial cellulose (e.g., ball-milling or mercerization), followed by acid hydrolysis or TEMPO oxidation [174].

1.6.4 Preparation of Cellulose Nanoyarn

Electrospinning is one of the simplest and most effective methods for producing micro- and nanofibers. In electrospinning, a high electrostatic voltage is imposed on a drop of polymer solution, held by its surface tension at the end of a capillary. The surface of the liquid is distorted into a conical shape known as the *Taylor cone*. Once the voltage exceeds a critical value, the electrostatic force overcomes the solution surface tension and a stable liquid jet is ejected from the cone tip. The solvent evaporates when the jet travels through the air, leaving ultrafine polymeric fibers that are collected on an electrically grounded target [175]. As a result, mats of tangled long filaments with diameters of 100–1000 nm are formed. Figure 1.12 is a schematic of the electrospinning process. The direct dissolution of cellulose is a difficult process. Therefore, cellulose nanofiber production using electrospinning requires a suitable solvent or chemical derivatization of the cellulose [7].

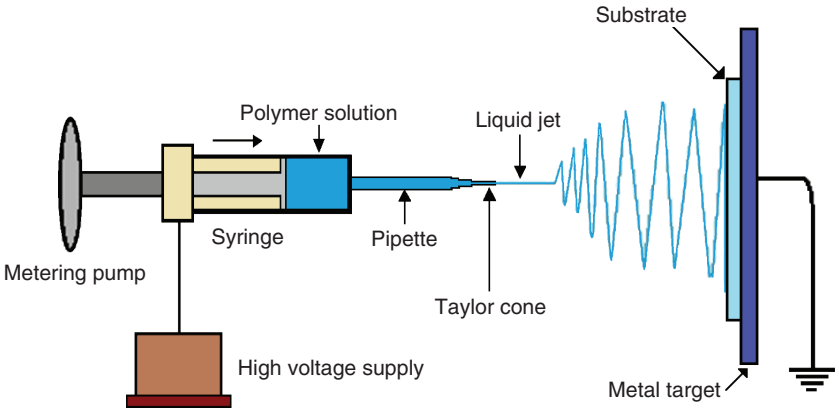

Figure 1.12 Schematic of electrospinning process.

Various systems for direct dissolution of cellulose without chemical derivatization have been studied, such as *N,N*-dimethylacetamide (DMAc)/LiCl [176], dimethyl sulfoxide (DMSO)/triethylamine/SO_2 [68], *N*-methylmorpholine-*N*-oxide (NMMO) [177], and NaOH/urea aqueous solution [178]. For example, to prepare CNY, cellulose has been dissolved in a LiCl/DMAc or NMMO/water system. After electrospinning, the CNY was coagulated in water and dried [67]. Investigation of the product indicated that coagulation with water immediately after collection of the CNY is necessary in order to obtain submicron-scale nano-filaments for both solvent systems. The DP of CNY is most likely close to that of conventional cellulose fibers. X-ray diffraction studies have revealed that CNY obtained from LiCl/DMAc are mostly amorphous, whereas the CNY from NMMO/water can be semicrystalline. Further, since the stretching stage of the amorphized fibers is absent in this process, the nanoyarn samples formed have relatively low mechanical characteristics. The resultant CNY mats are highly porous and can be used as blotting and filtering materials. Pure CNY has also been prepared by dissolving cellulose fibers in a mixture of ethylene diamine with a salt selected from the group composed of potassium thiocyanate, potassium iodide, and mixtures thereof [179].

Nanoyarn can also be produced from cellulose derivatives such as methylcellulose, ethylcellulose, nitrate cellulose, acetate cellulose, and acetate-butyrate cellulose. For instance, the electrospun nanoyarn from acetate cellulose can be produced using solutions of the initial polymer in acetic acid, acetone, or ethylacetate. The nanoyarn obtained from cellulose derivatives and produced from isotropic solvents such as acetone, dimethylformamide, ethanol, or methanol, and following electrospinning, exhibits reticulation due to the liquid crystalline structures of the solutions [180, 181]. Various parameters, such as the electric field strength, tip-to-collector distance, solution feed rate are generally used to control the morphological features of the electrospun nanofibers. The effects of these conditions on the production of nanoyarn with desirable characteristics and properties can be further examined, with a view to optimizing the process parameters [84].

1.7 Pretreatment

As known, two major problems often occur during the fibrillation process, and especially during the mechanical fibrillation of cellulose: (i) fibril aggregation, when slurry is pumped through the disintegration device and (ii) high energy consumption associated with fiber delamination, which often involves multiple passes through the disintegration device until efficient delamination of the cell wall is obtained. The high energy input is necessary in order to release the nanofibers and to overcome the interfibrillar hydrogen bonding [71]. According to Siró and Plackett [62], an efficient pretreatment helps to reduce energy consumption by 20–30-fold.

The choice of pretreatment method is dependent on the cellulose source and, to a lesser degree, on the desired morphology of the initial cellulose for further treatments. It is worth noting that appropriate pretreatment of cellulose fibers promotes accessibility, increases the inner surface, alters crystallinity, breaks hydrogen bonds, and boosts the reactivity of the cellulose; thus, it decreases the energy demand and facilitates the process of NC production [42, 64]. For instance, the pretreatment of plant materials promotes the complete or partial removal of noncellulose components (hemicellulose, lignin, etc.) and the isolation of individual fibers [36]. Pretreatment of tunicate involves the removal of the protein matrix, isolation of the mantel, and the isolation of individual cellulose fibrils [182]. Pretreatment of algae typically involves the removal of the matrix material of algae cell walls [48, 183], whereas pretreatment of bacterial NC is focused on the removal of bacteria and other impurities from the slurry [50]. Pretreatment is a very important step, because it can alter the structural organization, crystallinity, and polymorphism of the cellulose, as well as various properties of the pretreated feedstock [12]. Therefore, we wish to discuss the most efficient pretreatment methods to facilitate the cell wall delamination and release nano-sized fibrils.

1.7.1 Pulping Processes

Pulping is used to isolate fibers from wood or other plants and can be performed in two ways: mechanically or chemically. Mechanical pulping methods are energy consuming; however, they use almost the entire wood material. The production of wood fibers involves the grinding of round wood logs by a rotating sandstone cylinder; as a result, the wood fibers are scraped off. Another type of mechanical pulping leads to the production of refined wood pulp, which is obtained by feeding wood chips into the center of rotating refining disks in the presence of a water spray [184]. These mechanical treatments cause damage to the morphology and size of the wood fibers, and also reduce the cellulose DP and crystallinity [71].

In chemical kraft pulping, the plant materials are treated with a hot solution containing a mixture of sodium hydroxide and sulfide in a digester. In fact, approximately half of the wood is converted into pulp, while the other half is dissolved. Modern chemical pulping mills can efficiently recover the respective chemicals and burn the remaining residues. The combustion heat accounts for the entire energy consumption of the pulp mill. Other known types of the

chemical pulping are soda cooking, which uses sodium hydroxide only as a cooking chemical, and sulfite pulping by sulfite acid and its salts [36, 59, 184].

The chemical pulping process can be conducted also using sodium chlorite for selective oxidation of lignin, which gives a higher yield of delignified fibers compared to the conventional kraft pulping process. This improvement is explained by the difference in the chemical composition of the delignified fibers, and specifically of hemicelluloses. The correlation between the content of hemicelluloses and the efficiency of nanofibrillation has been shown in the work of Chaker *et al*. [185] and Iwamoto *et al*. [90]. These researchers have reported that the higher the hemicelluloses content in the fibers, the higher the yield of nanofibrillated material. The correlation between the extent of fibrillation and the hemicellulose content has been explained by consideration of the structural organization of CMFs and hemicelluloses within the cell wall. As mentioned previously, amorphous and hydrophilic hemicelluloses are tightly bonded to the CMFs via hydrogen bonds, and can act as physical barriers that keep the CMFs apart. Consequently, they prevent the aggregation and facilitate the fibrillation process [71].

1.7.2 Bleaching

In this process, the pulp can be bleached to remove the residual lignin and other impurities, without change in cellulose crystallinity or polymorphism. After the bleaching process, white cellulose with an improved aging resistance is obtained. Various bleaching agents can be used, such as hydrogen peroxide, oxygen, ozone, peracetic acid, sodium chlorite, chlorine, and chlorine dioxide [186–188]. Among the bleaching agents, oxygen and chlorine dioxide are the most popular. Further details about bleaching processes are given by Hubbe *et al*. [36].

1.7.3 Alkaline-Acid-Alkaline Pretreatment

This pretreatment includes three steps [64, 189, 190]: (i) soaking of plant fibers in 12–17.5 wt% sodium hydroxide for 2 h, in order to increase the fiber surface area and to make the fibers more susceptible to hydrolysis; (ii) treatment of the fibers with 1 M HA at 60–80 °C in order to hydrolyze the hemicelluloses; and (iii) treating the fibers with 2 wt% NaOH solution for 2 h at 60–80 °C to disrupt the lignin structure. According to Alemdar and Sain [92], after such pretreatment, the cellulose content in wheat straw increased from 43% to 84%.

1.7.4 Enzymatic Pretreatment

Enzymatic pretreatment is an environmentally friendly alternative to chemical pretreatment, which can be used to manufacture CNFs with significantly reduced energy consumption. Special enzymes, that is, ligninases, xylanases, and others, are capable of degrading lignin and hemicelluloses while maintaining cellulose. On the other hand, cellulolytic enzymes, that is, cellulases, help hydrolyze cellulosic fibers [191].

Based on their activity, cellulases can be divided into three groups [192]: (i) endoglucanases or β-1,4-endoglucanases (also called A- and B-type cellulases), which randomly hydrolyze accessible β-1,4-glucosidic bonds in noncrystalline

domains of cellulose, generating damaged fibers with new chain ends; (ii) exoglucanases (cellobiohydrolases), which are also called C- and D-type cellulases, which act on the chain termini to release soluble cellobiose as a major product; and (iii) β-glucosidases, which hydrolyze cellobiose to glucose. The commonly accepted cellulose hydrolysis mechanism suggests that these three types of cellulases work synergistically.

A combination of mild enzymatic hydrolysis with endoglucanase and high-pressure disintegration has been used to prepare CNFs from the bleached wood pulp [193, 194]. It was found that pretreatment with endoglucanase increases swelling of the pulp fibers in water and facilitates their disintegration, thus preventing the microfluidizer from blocking or clogging. The fibers pretreated with the lowest enzyme concentration (0.02%) were successfully disintegrated, while the molecular weight and fiber length were well preserved. As a result, mild enzymatic hydrolysis facilitates disintegration of pulp fibers into nanofibers. Compared with acidic pretreatment, the enzymatic pretreatment yielded homogeneous CNFs with greater aspect ratios.

The pretreatment of bleached sisal fibers with two types of commercial cellulases, endoglucanase or exoglucanase, has also been studied [166]. This pretreatment was performed using two different procedures, either before or after mechanical shearing in a microfluidizer. It was shown that, depending on the cellulase dose, the morphology of the prepared NC and its reinforcing effect can differ significantly. The use of endoglucanase leads to the formation of a mixture of CNFs and stiff rod-like nanoparticles, whereas exoglucanase preserves the web-like morphology of the CNFs regardless of the pretreatment sequence. Siddiqui *et al*. [72] reported that enzymatic pretreatment had a small effect on the resultant size of the CNFs, but at increased solid content the pretreated slurry could be passed through the HPH without blockage. The optimum size reduction of nanofibrils and smooth passing of the flow through the homogenizer was found for an enzyme concentration of 1%, while the obtained CNFs had diameters of 38–42 nm after three passes.

1.7.5 Ionic Liquids

ILs are a new group of organic salts that remain in the fluid state at temperatures below 100 °C. They have interesting and valuable properties such as non-flammability, and very low vapor pressure and thermal and chemical stability [195, 196]. The dissolution of cellulose in ILs allows the comprehensive utilization of this biopolymer through the combination of two major principles of green chemistry: (i) the use of environmentally preferable solvents and (ii) the use of a biorenewable source. It has been reported that cellulose can be dissolved in certain hydrophilic ILs, for example, in 1-butyl-3-methylimidazolium chloride (BmimCl) and 1-allyl-3-methylimidazolium chloride (AmimCl). The accepted dissolution mechanism is that IL cations attack the oxygen atoms, whereas IL anions associate with the protons of the hydroxyl groups of cellulose. These two interactions can eradicate the extensive network of hydrogen bonds, resulting in dissolution of cellulose. It has been found that microwave heating significantly accelerates the cellulose dissolution process in ILs. Cellulose can be easily

regenerated from its solution in ILs through addition of water, ethanol, or acetone, and transformed into NC [196].

To isolate CNFs from sugarcane bagasse, Li *et al*. [197] combined BmimCl pretreatment with HPH. The cellulose solution in the IL easily passed through the homogenizer without clogging. Afterwards, NC was precipitated from the solution by the addition of water and freeze dried. Good solubilization of the cellulose in the IL was observed for a dissolution temperature of 130 °C, microwave power of 400 W, and cellulose concentration in the IL of 1 wt%. Man *et al*. [162] prepared CNCs by treating MCC with $BmimHSO_4$. It was found that the IL can react with MCC in a similar manner to acid in acid hydrolysis, causing a hydrolytic cleavage of the glycosidic bonds between the AGU. As a result, needle-like CNCs with lengths of 50–300 nm and diameters of 14–22 nm were isolated. A high recovery yield (>90%) of $BmimHSO_4$ was reported after preparation of high crystalline CNCs by Tan *et al*. [198].

Gindl and Keckes [199] cast a solution of MCC in IL into a film, which was identified as a nanocomposite. In addition, Kilpeläinen *et al*. [200] suggested that cellulose could be precipitated from its solution in IL under various conditions, in order to obtain a wide range of morphologies. Sui *et al*. [201] formed cellulose nanofibers and nanoparticles by spraying cellulose solution in ILs, while Kadokawa *et al*. [202] used an IL to partially disrupt cellulosic material structure; this was followed by a polymerization reaction in the continuous phase.

Note that the IL is not consumed during treatment and can be recovered through various methods, such as evaporation, ion exchange, and reverse osmosis; moreover, the recovered IL can be reused [94].

1.7.6 Oxidation

TEMPO is a well-known reagent that is widely used for pretreatment of cellulose materials in the laboratory to reduce the energy consumption required for mechanical disintegration. It has been reported that, after TEMPO pretreatment of cellulose, the consumption of energy in HPH is dramatically decreased by a factor of over 100 [203]. TEMPO is a red-orange, sublimable solid with a melting point of 36–38 °C. It is a highly stable nitroxyl radical, which is used extensively in the selective oxidation of primary alcohols to corresponding aldehydes and carboxylic acids (Figure 1.13).

In an aqueous medium, TEMPO catalyzes the conversion of primary hydroxyl groups of carbohydrates into carboxyl groups in the presence of a primary oxidizing agent (e.g., sodium hypochlorite) and halogen salts (e.g., sodium bromide or sodium chloride) [204]. However, a side reaction (e.g., strong depolymerization

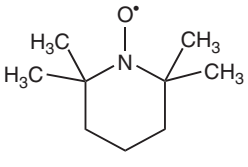

Figure 1.13 (2,2,6,6-Tetramethylpiperidin-1-oxyl) or (2,2,6,6-tetramethyl piperidin-1-oxidany) or TEMPO.

of the cellulose) occurs after cellulose TEMPO oxidation under alkaline conditions [205, 206]. Another side reaction of cellulose with a TEMPO system at pH > 7 is the formation of aldehyde groups, which reduce the thermal stability and cause discoloration of the oxidized cellulose after drying. Moreover, these groups disturb the individualization of the CMFs through the partial formation of hemi-acetal linkage between the fibrils.

To prevent the side reactions, the TEMPO pretreatment should be conducted under slightly acidic conditions (pH 6.0–6.5) and at temperatures of 50–60 °C. It has been found that, in these conditions, aldehyde groups are not formed and the depolymerization of the cellulose chains does not occur [203]. Schemes of TEMPO oxidation at alkaline and acidic pHs are shown in Figure 1.14. It is also believed that the reaction occurs on the surface and in the amorphous domains of the cellulose fibers. As the carboxyl content is increased to a certain amount, the cellulose begins to disperse in the aqueous solution, but the crystalline domains remain intact and can, therefore, be released [7].

The level of cellulose oxidation is critical in reducing the energy input and improving the degree of nanofibrillation as well as the transparency of the CNF suspension. Content of carboxyl group of approximately 300 μmol g^{-1} in the cellulose is required to provide an optimal CNF yield without clogging the homogenizer. However, the increase in the content of carboxyl groups above 500 μmol g^{-1} does not change the degree of nanofibrillation [207, 208]. Preparation of CNF can be controlled and optimized by monitoring the oxidation time and degree of oxidation, as well as the number of cycles through the homogenizer. A significant length reduction and improvement in the uniformity of CNF has been observed after TEMPO oxidation [209, 210].

CNCs with high carboxylic group content (1.66 mmol g^{-1}) have also been prepared from cotton linter pulp through direct ultrasonic-assisted TEMPO oxidation [211]. Microscopic observations have revealed CNCs with widths of 5–10 nm and lengths of 200–400 nm. It has been reported that oxidized CNCs form stable aqueous suspensions.

Recently, Carlsson *et al*. [212] prepared highly crystalline NC from *Cladophora* sp. algae via co-oxidant free TEMPO oxidation. These researchers demonstrated that the same degree of oxidation can be achieved within approximately the same time by replacing the co-oxidants with $TEMPO^+$ electrogeneration in a bulk electrolysis setup. It was shown that the oxidation does not affect the morphology, specific surface area, and pore characteristics of the obtained nanoparticles; however, a slight reduction in the DP value was observed.

Another route is the periodate oxidation of cellulose, which is followed by oxidation with sodium chlorite to convert aldehyde groups into carboxylic groups [213]. Compared to TEMPO oxidation, this oxidation route allows the introduction of a larger number of carboxylic groups, up to 3.5 mmol g^{-1}. It has been shown that the isolation of CNFs from highly oxidized cellulose can be achieved without applying any additional mechanical energy, other than that required to stir the fiber suspensions during the chemical treatments. The mechanism responsible for this "spontaneous" disintegration is most likely the repulsion of highly charged fibrils after a charge threshold is achieved at approximately 3 mmol g^{-1}.

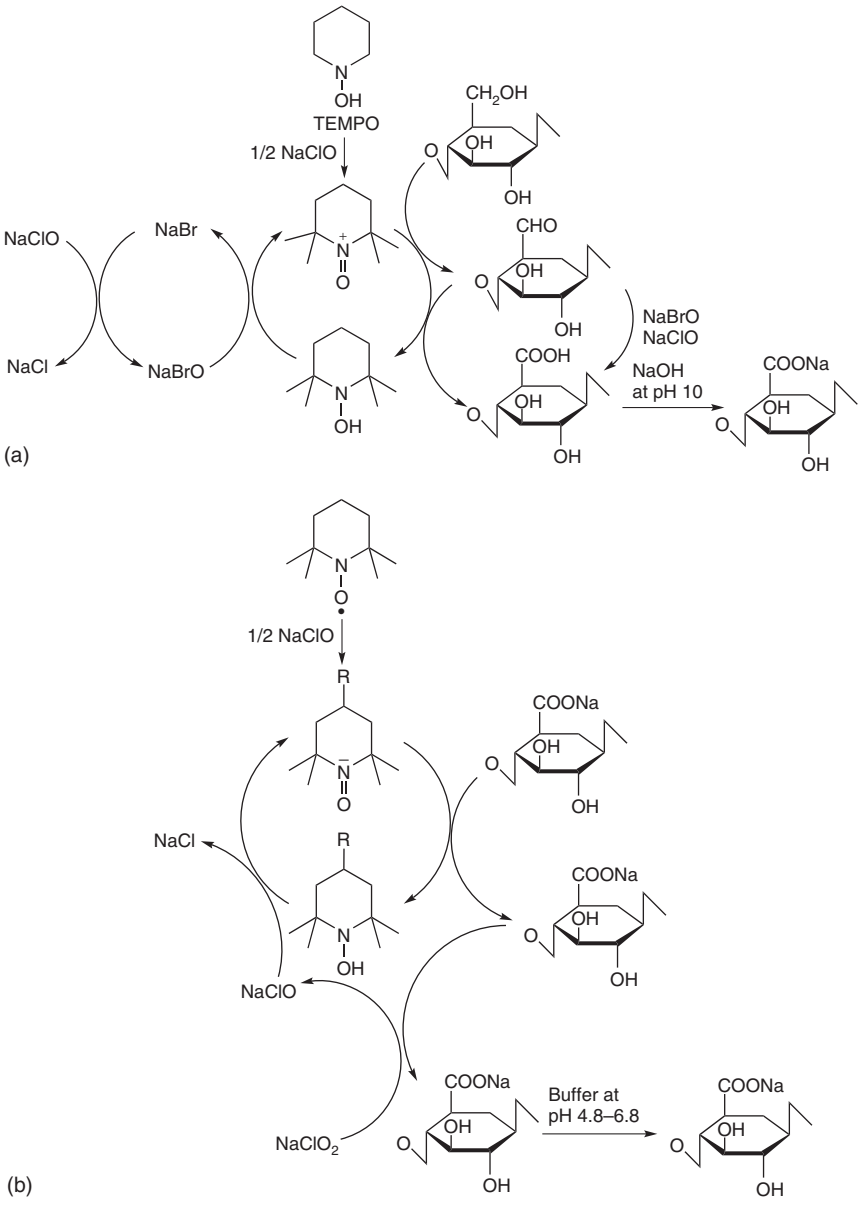

Figure 1.14 TEMPO-mediated oxidation of cellulose (a) at pH 10–11 and (b) pH 4.8–6.8. (Isogai *et al.* 2011 [203]. Reproduced with permission from Royal Society of Chemistry.)

1.7.7 Steam Explosion

Steam explosion is a promising pretreatment method for the extraction of cellulose fibers from plant biomass, which can be used either alone or in combination with high-pressure disintegration. This pretreatment is based on short-term "cooking" in a vapor phase at a temperature of 180–210 °C under steam pressure

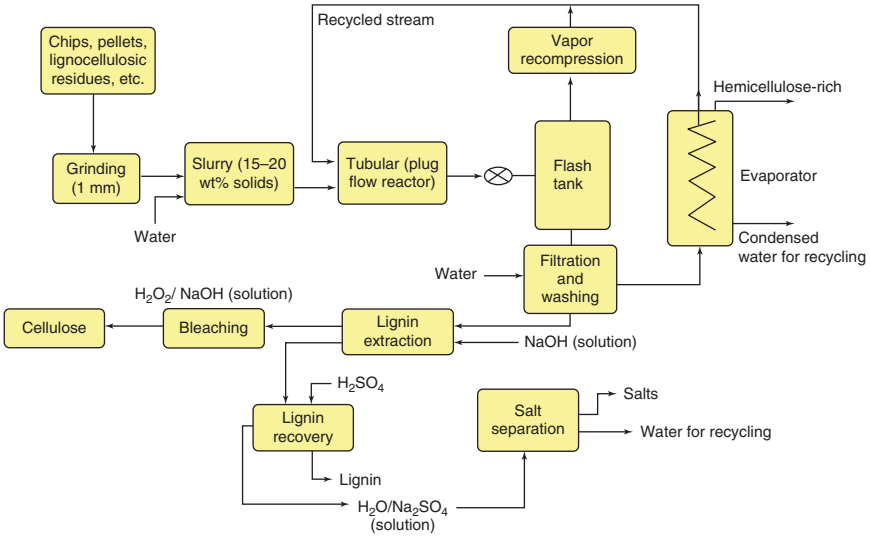

Figure 1.15 Process diagram of typical aqueous/steam explosion system. (Rebouillat and Pla [84], http://www.scirp.org/journal/PaperInformation.aspx?PaperID=29869. Used under CC-BY 4.0. https://creativecommons.org/licenses/by/4.0/.)

between 1 and 3.5 MPa. The pretreatment with the compressed steam is finished with an explosive decompression, during which the flash evaporation of water exerts a high force and causes the material to rupture. This effect results in a substantial breakdown of the plant material structure, namely, the hydrolysis of hemicelluloses, degradation of lignin, and fibrillation of fibers. The addition of certain chemicals, for example, SA or sodium hydroxide, promotes the enhancement of the pretreatment efficiency [214, 215]. Figure 1.15 is a process diagram of a typical steam explosion system.

Various plant materials have been steam exploded, including flax [216], cotton [217], wheat straw [218], bamboo [219], sunflower stalks [117], banana fibers [215], and pineapple leaf fibers [220]. The CNF yields obtained through this technique and the respective aspect ratios are higher than those of other conventional methods [215]. The advantages of steam explosion include low energy and chemical consumption, low environmental impact, and lower capital investment. However, this process should be repeated several times in order to efficiently release the fibrillated material [220, 221].

1.7.8 Other Pretreatments

Other, less used pretreatment methods include carboxymethylation and acetylation [85]. Aulin *et al*. [222] found that preliminary carboxymethylation produces highly charged cellulose that promotes the liberation of CNFs. Further, Taipale *et al*. [223] have reported that the energy required for the disintegration of cellulose fibers in a microfluidizer can be reduced by 2.5-fold after carboxymethylation.

The partial esterification of CNFs with acetyl groups decreases the hydrophilicity and enhances the chemical affinity between modified fibrils and nonpolar solvents. Tingaut *et al*. [224] found that the acetylation of nanofibrils to acetyl content above 4.5% prevents hornification of CNFs upon drying. Introducing of acetyl groups reduces the level of hydrogen bonds between nanofibrils, thus aiding their dispersion in a nonpolar polymeric matrix of nanocomposite materials. The capacity to store acetylated CNFs in dry form introduces possibilities for industrial-scale production.

Current research is focusing on the development of environmentally friendly, high-efficiency, and low-cost methods of NC isolation. One-step treatment or combinations of two or more methods have produced positive results in this regard. The combination of chemical treatment, mechanical refining, homogenization, and cryocrushing has been used to produce CNFs [189]. Using a combination of chemical and mechanical treatments, Jonoobi *et al*. [80] have obtained nanofibers exhibiting higher crystallinity and thermal stability than the initial cellulose material. Wang and Cheng [105] have found that the combination of highly intensive ultrasonication and high-pressure homogenization is effective for the fibrillation and production of uniform nanofibers. Ultrasonication has been proposed as an aid for the acid hydrolysis of cellulose used to obtain nanoparticles [172].

A method based on a combination of ball milling, acid hydrolysis, and sonication has been developed by Qua *et al*. [225], in order to obtain CNFs from MCC and flax fibers. Pretreatment of cellulose with enzymes or acids in combination with mechanical shearing has been performed by Henriksson *et al*. to extract NCFs with low energy consumption [193]. Spence *et al*. [226] have compared the properties of CNFs produced using microgrinding, homogenization, and microfluidization methods, and also considered energy utilization during fabrication. They concluded that CNFs produced by microgrinders and microfluidizers exhibit higher optical, physical, and mechanical properties compared to fibers produced using homogenization. It has also been reported that the combination of chemical pretreatment and HIUS improves the CNF yields of the initial cellulose materials [99, 106, 107].

1.8 Concluding Remarks

Cellulose is the most abundant natural polymer on Earth, and is an almost inexhaustible source for obtaining environmentally friendly and biocompatible products. Therefore, cellulose-based materials have become one of the most important bioresources in the twenty-first century. The unique hierarchical structure of cellulose provides the possibility for isolation of micro-(CMFs) and nanofibrils (CNFs), crystalline (CNCs), and amorphous (ANC) nanoparticles. This characteristic also facilitates production of the nanoyarn.

The properties of the various types of extracted NC depend on the source and preparation technique. CMFs and CNFs are commonly produced via mechanical treatment using devices such as HPH, microfluidizers, microgrinders, and

high-intensity ultrasound dispersers. However, these mechanical procedures involve multiple passes through the disintegration device and require a high consumption of energy in order to overcome the interfibrillar hydrogen bonds, perform efficient delamination of cellulose fibers and release the free nanofibers. Special pretreatments of the pulp are necessary in order to reduce the energy consumption and prevent fibril aggregation, when the slurry is pumped through the disintegration device. These pretreatments include biological, physico-chemical, chemical, physical, and mechanical procedures, or combinations thereof.

On the other hand, the main preparation technique commonly used to produce the CNCs is acid hydrolysis. The shapes, sizes, and properties of isolated CNCs depend on the hydrolysis conditions, such as time, temperature, concentration, and acid type, as well as the acid/cellulose ratio. The pretreatment and preparation techniques used to produce NC must be conducted under controlled conditions. Then, NC can be obtained not only at high yield, but also with the desired size and properties. The preparation methods of some other NC types, for example, amorphous nanoparticles and nanoyarn, have also been shortly described in this chapter.

The characterization of various types of NC, along with their application in the production of nanocomposites, nano-hydrogels, nano-dispersions, nano-foams, and other nanomaterials that can be used in papermaking, plastics, textile industry, packaging, coating, cosmetics, medicine, and pharmaceuticals, are discussed in the following chapters.

References

1 Miao, Q., Chen, L., Huang, L., Tian, C., Zheng, L., and Ni, Y. (2014) A process for enhancing the accessibility and reactivity of hardwood kraft-based dissolving pulp for viscose rayon production by cellulose treatment. *Bioresour. Technol.*, **154**, 109–113.

2 Mtibe, A., Linda, Z., Linganisoa, L.Z., Mathew, A.P., Oksman, K., John, M.J., and Anandjiwala, R.D. (2015) A comparative study on properties of micro and nanopapers produced from cellulose and cellulose nanofibers. *Carbohydr. Polym.*, **118**, 1–8.

3 Neto, W.P.F., Silvério, H.A., Dantas, N.O., and Pasquini, D. (2013) Extraction and characterization of cellulose nanocrystals from agro-industrial residue—Soy hulls. *Ind. Crops Prod.*, **42**, 480–488.

4 Habibi, Y. (2014) Key advances in the chemical modification of nanocelluloses. *Chem. Soc. Rev.*, **43** (5), 1519–1542.

5 Brown, R.M. (1996) The biosynthesis of cellulose. *J. Macromol. Sci. Part A Pure Appl. Chem.*, **A33** (10), 1345–1373.

6 Saxena, I.M. and Brown, R.M. (2005) Cellulose biosynthesis: current views and evolving concepts. *Ann. Bot.*, **96** (1), 9–21.

7 Dufresne, A. (2012) *Nano-cellulose: from Nature to High Performance Tailored Materials*, Walter de Gruyter GmbH, Berlin/Boston, MA.

8 Ioelovich, M. (2008) Cellulose as a nanostructured polymer: a short review. *Bioresources*, **3** (4), 1403–1418.
9 Preston, R.D. (1974) *The Physical Biology of Plant Cell Walls*, Chapman & Hall, London.
10 Ioelovich, M. (2013) *Plant Biomass as a Renewable Source of Biofuels and Biochemicals*, Saarbrücken Lap Lambert Academic Publishing.
11 Ioelovich, M. (2013) Nanoparticles of amorphous cellulose and their properties. *Am. J. Nanosci. Nanotechnol.*, **1** (1), 41–45.
12 Mariano, M., El Kissi, N., and Dufresne, A. (2014) Cellulose nanocrystals and related nanocomposites: review of some properties and challenges. *J. Polym. Sci., Part B: Polym. Phys.*, **52**, 791–806.
13 Zimmermann, T., Pohlerand, E., and Geiger, T. (2004) Cellulose fibrils for polymer reinforcement. *Adv. Eng. Mater.*, **9** (6), 754–761.
14 de Menezes, A.J., Siqueira, G., Curvelo, A.A.S., and Dufresne, A. (2009) Extrusion and characterization of functionalized cellulose whiskers reinforced polyethylene nanocomposites. *Polymer*, **50** (19), 4552–4563.
15 Nishino, T. (2004) in *Green Composites: Polymer Composites and the Environment* (eds C. Baillie and R. Jayasinghe), CRC Press, Boca Raton, FL, New York, pp. 61–79.
16 Kalia, S., Dufresne, A., Cherian, B.M., Kaith, B.S., Avérous, L., Njuguna, J., and Nassiopoulos, E. (2011) Cellulose-based bio-and nanocomposites: a review. *Int. J. Polym. Sci.*, **2011**, 1–35.
17 Moon, R.J., Martini, A., Nairn, J., Simonsen, J., and Youngblood, J. (2011) Cellulose nanomaterials review: structure, properties and nanocomposites. *Chem. Soc. Rev.*, **40** (7), 3941–3994.
18 Ioelovich, M. (1991) Study of cellulose cocrystallization process during its isolation from plants. *Wood Chem.*, **4**, 27–33.
19 Ioelovich, M. (2014) *Cellulose–Nanostructured Natural Polymer*, Lambert Academic Publishing, Saarbrücken.
20 Meyer, K.H. and Misch, L. (1937) Positions des atomes dans le nouveau modèle spatial de la cellulose. *Helv. Chim. Acta*, **20** (1), 232–244.
21 Gardner, K.H. and Blackwell, J. (1974) The structure of native cellulose. *Biopolymers*, **13** (10), 1975–2001.
22 Zugenmaier, P. (2001) Conformation and packing of various crystalline cellulose fibers. *Prog. Polym. Sci.*, **26** (9), 1341–1417.
23 Zugenmaier, P. (2008) *Crystalline Cellulose and Cellulose Derivatives: Characterization and Structures*, Springer-Verlag, Berlin/Heidelberg.
24 Ding, S.Y. and Himmel, M.F. (2006) The maize primary cell wall microfibril: a new model derived from direct visualization. *J. Agric. Food Chem.*, **54** (3), 597–606.
25 Yang, B., Dai, Z., Din, S.Y., and Wyman, C.E. (2011) Enzymatic hydrolysis of cellulosic biomass. *Biofuels*, **2** (4), 421–450.
26 Krässig, H.A. (1993) *Cellulose, Structure, Accessibility and Reactivity*, Gordon and Breach Publishers, Amsterdam.
27 Ioelovich, M., Leykin, A., and Figovsky, O. (2010) Study of cellulose paracrystallinity. *Bioresources*, **5** (3), 1393–1407.

28 Klemm, D., Heublein, B., Fink, H.P., and Bohn, A. (2005) Cellulose: fascinating biopolymer and sustainable raw material. *Angew. Chem. Int. Ed.*, **44**, 2–37.

29 Hearle, J.W.S. (1863) The fine structure of fibers and crystalline polymers. 1. Fringed fibril structure. *J. Appl. Polym. Sci.*, **7** (4), 1175–1192.

30 Wilkie, J.S. (1961) Carl Nägeli and the fine structure of living matter. *Nature*, **190** (4782), 1145–1150.

31 Zugenmaier, P. (2009) Contribution to the historical development of macromolecular chemistry–exemplified on cellulose. *Cellul. Chem. Technol.*, **4** (9–10), 351–378.

32 Pakzad, A., Simonsen, J., Heiden, P.A., and Yassar, R.S. (2012) Size effects on the nanomechanical properties of cellulose I nanocrystals. *J. Mater. Res.*, **27** (3), 528–536.

33 Ioelovich, M. (2015) Recent findings and the energetic potential of plant biomass as a renewable source of biofuels – a review. *Bioresources*, **10** (1), 1879–1914.

34 Habibi, Y., Lucia, L.A., and Rojas, O.J. (2010) Cellulose nanocrystals: chemistry, self-assembly, and applications. *Chem. Rev.*, **110**, 3479–3500.

35 Abrahama, E., Deepa, B.P., Pothen, L.A., Cintil, J., Thomas, S., John, M.J., Anandjiwala, R., and Narine, S.S. (2013) Environmental friendly method for the extraction of coir fibre and isolation of nanofibre. *Carbohydr. Polym.*, **92** (2), 1477–1483.

36 Hubbe, M.A., Rojas, O.J., Lucia, L.A., and Sain, M. (2008) Cellulosic nanocomposites: a review. *Bioresources*, **3** (3), 929–980.

37 Emanuel, M.F., Ricardo, A.P., Mano, J.F., and Reisa, R.L. (2013) Bionanocomposites from lignocellulosic resources: properties, applications and future trends for their use in the biomedical field. *Prog. Polym. Sci.*, **38** (10–11), 1415–1441.

38 Elazzouzi-Hafraoui, S., Nishiyama, Y., Putaux, J.-L., Heux, L., Dubreuil, F., and Rochas, C. (2008) The shape and size distribution of crystalline nanoparticles prepared by acid hydrolysis of native cellulose. *Biomacromolecules*, **9** (1), 57–65.

39 Iwamoto, S., Isogai, A., and Iwata, T. (2011) Structure and mechanical properties of wet-spun fibers made from natural cellulose nanofibers. *Biomacromolecules*, **12** (3), 831–836.

40 Kimura, S. and Itoh, T. (1996) New cellulose synthesizing complexes (terminal complexes) involved in animal cellulose biosynthesis in the tunicate *Metandrocarpa uedai*. *Protoplasma*, **194** (3–4), 151–163.

41 Peng, B.L., Dhar, N., Liu, H.L., and Tam, K.C. (2011) Chemistry and applications of nanocrystalline cellulose and its derivatives: a nanotechnology perspective. *Can. J. Chem. Eng.*, **89** (5), 1191–1206.

42 Šturcová, A., Davies, G.R., and Eichhorn, S.J. (2005) Elastic modulus and stress-transfer properties of tunicate cellulose whiskers. *Biomacromolecules*, **6** (2), 1055–1061.

43 Zhao, Y., Zhang, Y., Lindström, M.E., and Li, J. (2014) Tunicate cellulose nanocrystals: preparation, neat films and nanocomposite films with glucomannans. *Carbohydr. Polym.*, **117**, 286–296.

44 Imai, T. and Sugiyama, J. (1998) Nanodomains of I_α and I_β cellulose in algal microfibrils. *Macromolecules*, **31** (18), 6275–6279.

45 Kim, N.-H., Herth, W., Vuong, R., and Chanzy, H. (1996) The cellulose system in the cell wall of *Micrasterias*. *J. Struct. Biol.*, **117** (3), 195–203.

46 Sugiyama, J., Harada, H., Fujiyoshi, Y., and Uyeda, N. (1985) Lattice images from ultrathin sections of cellulose microfibrils in the cell wall of Valonia macrophysa Kütz. *Planta*, **166** (2), 161–168.

47 Hua, K., Stromme, M., Mihranyam, A., and Ferraz, N. (2015) Nanocellulose from green algae modulates the in vitro inflammatory response of monocytes/macrophages. *Cellulose*, **22**, 3673–3688.

48 Hanley, S.J., Revol, J.-F., Godbout, L., and Gray, D.G. (1997) Atomic force microscopy and transmission electron microscopy of cellulose from *Micrasterias denticulata*; evidence for a chiral helical microfibril twist. *Cellulose*, **4** (3), 209–220.

49 Revol, J.F. (1982) On the cross-sectional shape of cellulose crystallites in *Valonia ventricosa*. *Carbohydr. Polym.*, **2** (2), 123–134.

50 Ashjaran, A., Yazdanshenas, M.E., Rashidi, A., Khajavi, R., and Rezaee, A. (2013) Overview of bio nanofabric from bacterial cellulose. *J. Text. Inst.*, **104** (2), 121–131.

51 Kalita, R.D., Nath, Y., Ochubiojo, M.E., and Buragohain, A.K. (2013) Extraction and characterization of microcrystalline cellulose from fodder grass; *Setaria glauca* (L.) P. Beauv, and its potential as a drug delivery vehicle for isoniazid, a first line antituberculosis drug. *Colloids Surf., B*, **108**, 85–89.

52 Dufresne, A., Cavaillé, J.Y., and Vignon, M.R. (1997) Mechanical behavior of sheets prepared from sugar beet cellulose microfibrils. *J. Appl. Polym. Sci.*, **64** (6), 1185–1194.

53 Pelissari, F.M., Sobral, P.J.A., and Menegalli, F.C. (2014) Isolation and characterization of cellulose nanofibers from banana peels. *Cellulose*, **21** (1), 417–432.

54 Habibi, Y., Goffin, A.L., Schiltz, N., Duquesne, E., Dubois, P., and Dufresne, A. (2008) Bionanocomposites based on poly(*E*-caprolactone)-grafted cellulose nanocrystals by ring-opening polymerization. *J. Mater. Chem.*, **18**, 5002–5010.

55 Frento, A., Henriksoon, M.W., and Walkenström, P. (2007) Electrospinning of cellulose-based nanofibers. *J. Appl. Polym. Sci.*, **103**, 1473–1482.

56 Ahola, S., Turon, X., Osterberg, M., Laine, J., and Rojas, O. (2008) Enzymatic hydrolysis of native cellulose nanofibrils and other cellulose model films: effect of surface structure. *Langmuir*, **24** (20), 11592–11599.

57 Henriksson, M., Berglund, L.A., Isaksson, P., Lindström, T., and Nishino, T. (2008) Cellulose nanopaper structures of high toughness. *Biomacromolecules*, **9** (6), 1579–1585.

58 Abe, K., Iwamoto, S., and Yano, H. (2007) Obtaining cellulose nanofibers with a uniform width of 15 nm from wood. *Biomacromolecules*, **8** (10), 3276–3278.

59 Abdul Khalil, H.P.S., Bhat, A.H., and Ireana Yusra, A.F. (2012) Green composites from sustainable cellulose nanofibrils: a review. *Carbohydr. Polym.*, **87**, 963–979.

60 Davoudpour, Y., Hossain, S., Abdul Khalil, H.P.S., Mohamad Haafiz, M.K., Mohd Ishak, Z.A., Hassan, A., and Sarker, Z.I. (2015) Optimization of high pressure homogenization parameters for the isolation of cellulosic nanofibers using response surface methodology. *Ind. Crops Prod.*, **74**, 381–387.

61 Ioelovich, M. (2014) Peculiarities of cellulose nanoparticles. *Tappi J.*, **13** (5), 45–52.

62 Siró, I. and Plackett, D. (2010) Microfibrillated cellulose and new nanocomposite materials: a review. *Cellulose*, **17** (3), 459–494.

63 Missoum, K., Belgacem, M.N., and Bras, J. (2013) Nanofibrillated cellulose surface modification: a review. *Materials*, **6**, 1745–1766.

64 Abdul Khalil, H., Davoudpour, Y., Islam, M.N., Mustapha, A., Sudesh, K., Dungani, R., and Jawaid, M. (2014) Production and modification of nanofibrillated cellulose using various mechanical processes: a review. *Carbohydr. Polym.*, **99**, 649–665.

65 Tashiro, K. and Kobayashi, M. (1991) Theoretical evaluation of three-dimensional elastic constants of native and regenerated celluloses: role of hydrogen bonds. *Polymer*, **32** (8), 1516–1526.

66 Rusli, R. and Eichhorn, S.J. (2008) Determination of the stiffness of cellulose nanowhiskers and the fiber-matrix interface in a nanocomposite using Raman spectroscopy. *Appl. Phys. Lett.*, **93** (3), 033111.

67 Kim, C.W., Kim, D.S., Kang, S.Y., Marquez, M., and Joo, Y.L. (2006) Structural studies of electrospun cellulose nanofibers. *Polymer*, **47** (14), 5097–5107.

68 Quan, S.L., Kang, S.G., and Chin, I.J. (2010) Characterization of cellulose fibers electrospun using ionic liquid. *Cellulose*, **17** (2), 223–230.

69 Stylianopoulos, T., Kokonou, M., Michael, S., Tryfonos, A., Rebholz, C., Odysseos, A.D., and Doumanidis, C. (2012) Tensile mechanical properties and hydraulic permeabilities of electrospun cellulose acetate fiber meshes. *J. Biomed. Mater. Res.*, **100** (8), 2222–2230.

70 Müller, R., Jacobs, C., and Kayser, O. (2001) Nanosuspensions as particulate drug formulations in therapy: rationale for development and what we can expect for the future. *Adv. Drug Delivery Rev.*, **47** (1), 3–19.

71 Kalia, S., Boufi, S., Celli, A., and Kango, S. (2014) Nanofibrillated cellulose: surface modification and potential applications. *Colloid. Polym. Sci.*, **292** (1), 5–31.

72 Siddiqui, N., Mills, R.H., Gardner, D.J., and Bousfield, D. (2011) Production and characterization of cellulose nanofibers from wood pulp. *J. Adhes. Sci. Technol.*, **25** (6–7), 709–721.

73 Wang, Y., Li, J., Wang, Q., Wang, F., and Kong, L. (2013) Homogeneous isolation of nanocellulose from cotton cellulose by high pressure homogenization. *J. Mater. Sci. Chem. Eng.*, **1** (05), 49–52.

74 Wang, Y., Wei, X., Li, J., Wang, F., Wang, Q., Chen, J., and Kong, L. (2015) Study on nanocellulose by high pressure homogenization in homogeneous isolation. *Fibers Polym.*, **16** (3), 572–578.

75 Chirayil, C.J., Joy, J., Mathew, L., Mozetic, M., Koetz, J., and Thomas, S. (2014) Isolation and characterization of cellulose nanofibrils from *Helicteres isora* plant. *Ind. Crops Prod.*, **59**, 27–34.

76 Winuprasith, T. and Suphantharika, M. (2013) Microfibrillated cellulose from mangosteen (*Garcinia mangostana* L.) rind: preparation, characterization, and evaluation as an emulsion stabilizer. *Food Hydrocolloids*, **32** (2), 383–394.

77 Leitner, J., Hinterstoisser, B., Wastyn, M., Keckes, J., and Gindl, W. (2007) Sugar beet cellulose nanofibril-reinforced composites. *Cellulose*, **14** (5), 419–425.

78 Habibi, Y., Mahrouz, M., and Vignon, M.R. (2009) Microfibrillated cellulose from the peel of prickly pear fruits. *Food Chem.*, **115** (2), 423–429.

79 Jonoobi, M., Harun, J., Mathew, A.P., Hussein, M.Z.B., and Oksman, K. (2010) Preparation of cellulose nanofibers with hydrophobic surface characteristics. *Cellulose*, **17** (2), 299–307.

80 Jonoobi, M., Harun, J., Shakeri, A., Misra, M., and Oksman, K. (2009) Chemical composition, crystallinity, and thermal degradation of bleached and unbleached kenaf bast (*Hibiscus cannabinus*) pulp and nanofibres. *Bioresources*, **4** (2), 626–639.

81 Jonoobi, M., Harun, J., Tahir, P.M., Shakerib, A., SaifulAzry, S., and Makinejad, M.D. (2011) Physicochemical characterization of pulp and nanofibers from kenaf stem. *Mater. Lett.*, **65** (7), 1098–1100.

82 Jonoobi, M., Harun, J., Tahir, P.M., Zaini, L.H., SaifulAzry, S., and Makinejad, M.D. (2010) Characteristics of nanofibers extracted from kenaf core. *Bioresources*, **5** (4), 2556–2566.

83 Zimmermann, T., Bordeanu, N., and Strub, E. (2010) Properties of nanofibrillated cellulose from different raw materials and its reinforcement potential. *Carbohydr. Polym.*, **79**, 1086–1093.

84 Rebouillat, S. and Pla, F. (2013) State of art manufacturing and engineering of nanocellulose: a review of available data and industrial application. *J. Biomater. Nanobiotechnol.*, **4**, 165–188.

85 Lavoine, N., Desloges, I., Dufresne, A., and Bras, J. (2012) Microfibrillated cellulose–its barrier properties and applications in cellulosic materials: a review. *Carbohydr. Polym.*, **90** (2), 735–764.

86 Lee, S.Y., Chun, S.J., Kang, I.A., and Park, J.Y.D. (2009) Preparation of cellulose nanofibers by high-pressure homogenizer and cellulose-based composite films. *J. Indian Eng. Chem.*, **15**, 50–55.

87 Ferrer, A., Filpponen, I., Rodríguez, A., Laine, J., and Rojas, O.J. (2012) Valorization of residual Empty Palm Fruit Bunch Fibers (EPFBF) by microfluidization: production of nanofibrillated cellulose and EPFBF nanopaper. *Bioresour. Technol.*, **125**, 249–255.

88 Wang, Q.Q., Zhu, J.Y., Gleisner, R., Kuster, T.A., Baxa, U., and McNeil, S.E. (2012) Morphological development of cellulose fibrils of a bleached eucalyptus pulp by mechanical fibrillation. *Cellulose*, **19**, 1631–1643.

89 Hassan, M.L., Mathew, A.P., Hassan, E.A., El-Wakil, N.A., and Oksman, K. (2012) Nanofibers from bagasse and rice straw: process optimization and properties. *Wood Sci. Technol.*, **46**, 193–205.

90 Iwamoto, S., Nakagaito, A.N., Yano, H., and Nogi, M. (2005) Optically transparent composites reinforced with plant fiber-based nanofibers. *Appl. Phys. A*, **81** (6), 1109–1112.

91 Iwamoto, S., Nakagaito, A.N., and Yano, H. (2007) Nano-fibrillation of pulp fibers for the processing of transparent nanocomposites. *Appl. Phys. A*, **89**, 461–466.

92 Alemdar, A. and Sain, M. (2008) Isolation and characterization of nanofibers from agricultural residues: wheat straw and soy hulls. *Bioresour. Technol.*, **9**, 1664–1671.

93 Chakraborty, A., Sain, M., and Kortschot, M. (2006) Wood Microfibres-Effective Reinforcing Agents for Composites. SAE Technical Paper, 2006-01-0106.

94 Frone, A.N., Panaitescu, D.M., and Donescu, D. (2011) Some aspects concerning the isolation of cellulose micro-and nano-fibers. *UPB Sci. Bull., Ser. B: Chem. Mater. Sci.*, **73** (2), 133–152.

95 Wang, B. and Sain, M. (2007) Dispersion of soybean stock-based nanofiber in a plastic matrix. *Polym. Int.*, **56**, 538–546.

96 Wang, B. and Sain, M. (2007) Isolation of nanofibers from soybean source and their reinforcing capability on synthetic polymers. *Compos. Sci. Technol.*, **67**, 2521–2527.

97 Chen, P., Yu, H., Liu, Y., Chen, W., Wang, X., and Ouyang, M. (2013) Concentration effects on the isolation and dynamic rheological behavior of cellulose nanofibers via ultrasonic processing. *Cellulose*, **20** (1), 149–157.

98 Frone, A.N., Panaitescu, D.M., Spataru, D.D., Radovici, C., Trusca, R., and Somoghi, R. (2011) Preparation and characterization of PVA composites with cellulose nanofibers obtained by ultrasonication. *Bioresources*, **6** (1), 487–512.

99 Johnson, R., Zink-Sharp, A., Renneckar, S., and Glasser, W. (2009) A new bio-based nanocomposite: fibrillated TEMPO-oxidized celluloses in hydroxypropylcellulose matrix. *Cellulose*, **16** (2), 227–238.

100 Qua, E.H., Hornsby, P.R., Sharma, H.S.S., and Lyons, G. (2011) Preparation and characterisation of cellulose nanofibres. *J. Mater. Sci.*, **46** (18), 6029–6045.

101 Shaoli, Y. and Zhiming, L. (2012) Preparation technology optimization analysis of bamboo pulp nano-cellulose. *Guangdong Chem. Ind.*, **15**, 036.

102 Khawas, P. and Deka, S.C. (2016) Isolation and characterization of cellulose nanofibers from culinary banana peel using high-intensity ultrasonication combined with chemical treatment. *Carbohydr. Polym.*, **137**, 608–616.

103 Rezanezhad, S., Nazanezhad, N., and Asadpur, G. (2013) Isolation of nanocellulose from rice wast via ultrasonication. *Lignocellulose*, **2** (1), 282–291.

104 Cheng, Q., Wang, S., and Han, Q. (2010) Novel process for isolating fibrils from cellulose fibers by high-intensity ultrasonication. II. Fibril characterization. *J. Appl. Polym. Sci.*, **115**, 2756–2762.

105 Wang, S. and Cheng, Q. (2009) A novel process to isolate fibrils from cellulose fibers by high-intensity ultrasonication, part 1: process optimization. *J. Appl. Polym. Sci.*, **113** (2), 1270–1275.

106 Mishra, S.P., Manent, A.S., Chabot, B., and Daneault, C. (2012) Production of nanocellulose from native cellulose-various options utilizing ultrasound. *Bioresources*, **7** (1), 422–436.

107 Chen, W., Yu, H., Liu, Y., Zhang, M., and Chen, P. (2011) Isolation and characterization of cellulose nanofibers from four plant cellulose fibers using a chemical-ultrasonic process. *Cellulose*, **18**, 433–442.

108 Araki, J., Wada, M., Kuga, S., and Okano, T. (1998) Low properties of microcrystalline cellulose suspension prepared by acid treatment of native cellulose. *Colloids Surf., A*, **142** (1), 75–82.

109 Yu, H., Qin, Z., Liang, B., Liu, N., Zhou, Z., and Chen, L. (2013) Facile extraction of thermally stable cellulose nanocrystals with a high yield of 93% through hydrochloric acid hydrolysis under hydrothermal conditions. *J. Mater. Chem. A*, **1** (12), 3938–3944.

110 Camarero Espinosa, S., Kuhnt, T., Foster, E.J., and Weder, C. (2013) Isolation of thermally stable cellulose nanocrystals by phosphoric acid hydrolysis. *Biomacromolecules*, **14** (4), 1223–1230.

111 Koshizawa, T. (1960) Degradation of wood cellulose and cotton linters in phosphoric acid. *Jpn. Tappi J.*, **14** (7), 455–458, 475.

112 Um, B.H., Karim, M.N., and Henk, L.L. (2003) Effect of sulfuric and phosphoric acid pretreatments on enzymatic hydrolysis of corn stover. *Appl. Biochem. Biotechnol.*, **105** (1–3), 115–125.

113 Filson, P.B. and Dawson-Andoh, B.E. (2009) Sono-chemical preparation of cellulose nanocrystals from lignocellulose derived materials. *Bioresour. Technol.*, **100** (7), 2259–2264.

114 Liu, D., Zhong, T., Chang, P.R., Li, K., and Wu, Q. (2010) Starch composites reinforced by bamboo cellulosic crystals. *Bioresour. Technol.*, **101**, 2529–2536.

115 Yan, C.F., Yu, H.Y., and Yao, J.M. (2015) One-step extraction and functionalization of cellulose nanospheres from lyocell fibers with cellulose II crystal structure. *Cellulose*, **22**, 3773–3788.

116 Braun, B. and Dorgan, J.R. (2008) Single-step method for the isolation and surface functionalization of cellulosic nanowhiskers. *Biomacromolecules*, **10** (2), 334–341.

117 Ruiz, E., Cara, C., Manzanares, P., Ballesteros, M., and Castro, E. (2008) Evaluation of steam explosion pre-treatment for enzymatic hydrolysis of sunflower stalks. *Enzyme Microb. Technol.*, **42** (2), 160–166.

118 Bai, W., Holbery, J., and Li, K.C. (2009) A technique for production of nanocrystalline cellulose with a narrow size distribution. *Cellulose*, **16** (3), 455–465.

119 de Souza Lima, M.M. and Borsali, R. (2002) Static and dynamic light scattering from polyelectrolyte microcrystal cellulose. *Langmuir*, **18** (4), 992–996.

120 Lu, P. and Hsieh, Y.L. (2010) Preparation and properties of cellulose nanocrystals: rods, spheres, and network. *Carbohydr. Polym.*, **82** (5), 329–336.

121 Roman, M. and Winter, W.T. (2004) Effect of sulfate groups from sulfuric acid hydrolysis on the thermal degradation behavior of bacterial cellulose. *Biomacromolecules*, **5** (5), 1671–1677.

122 Kargarzadeh, H., Ahmad, I., Abdullah, I., Dufresne, A., Zainudin, S.Y., and Sheltami, R.M. (2012) Effects of hydrolysis conditions on the morphology,

crystallinity, and thermal stability of cellulose nanocrystals extracted from kenaf bast fibers. *Cellulose*, **19** (3), 855–866.

123 Bondeson, D., Mathew, A., and Oksman, K. (2006) Optimization of the isolation of nanocrystal from microcrystalline cellulose by acid hydrolysis. *Cellulose*, **13** (2), 171–180.

124 Dong, X.M., Revol, J.F., and Gray, D.G. (1998) Effect of microcrystallite preparation conditions on the formation of colloid crystals of cellulose. *Cellulose*, **5** (1), 19–32.

125 Martínez-Sanz, M., Lopez-Rubio, A., and Lagaron, J.M. (2011) Optimization of the nanofabrication by acid hydrolysis of bacterial cellulose nanowhiskers. *Carbohydr. Polym.*, **85** (1), 228–236.

126 Ioelovich, M. (2012) Optimal conditions for isolation of nano-crystalline cellulose particles. *Nanosci. Nanotechnol.*, **2** (2), 9–13.

127 Ioelovich, M. and Leykin, A. (2006) Formation of nanostructure of microcrystalline cellulose. *Cellul. Chem. Technol.*, **40** (5), 313–317.

128 Li, Y. and Ragauskas, A.J. (2011) Cellulose nano whiskers as a reinforcing filler in polyurethanes. *Algae*, **75** (80), 10–15.

129 Guo, J., Guo, X., Wang, S., and Yin, Y. (2016) Effects of ultrasonic treatment during acid hydrolysis on the yield, particle size and structure of cellulose nanocrystals. *Carbohydr. Polym.*, **135**, 248–255.

130 Mondragon, G., Fernandes, S., Retegi, A., Peña, C., Algar, I., Eceiza, A., and Arbelaiz, A. (2014) A common strategy to extracting cellulose nanoentities from different plants. *Ind. Crops Prod.*, **55**, 140–148.

131 Nascimento, D.M., Almeida, J.S., Dias, A.F., Figueirêdo, M.C.B., Morais, J.P.S., Feitosa, J.P.A., and Rosa, M.F. (2014) A novel green approach for the preparation of cellulose nanowhiskers from white coir. *Carbohydr. Polym.*, **110**, 456–463.

132 Chen, D., Lawton, D., Thompson, M.R., and Liu, Q. (2012) Biocomposites reinforced with cellulose nanocrystals drived from potato peel wast. *Carbohydr. Polym.*, **90**, 709–716.

133 Wu, Q., Meng, Y., Concha, K., Wang, S., Li, Y., Ma, L., and Fu, S. (2013) Influence of temperature and humidity on nano-mechanical properties of cellulose nanocrystal films made from switchgrass and cotton. *Ind. Crops Prod.*, **48**, 28–35.

134 Silvério, H.A., Flauzino Neto, W.P.F., Dantas, N.O., and Pasquini, D. (2013) Extraction and characterization of cellulose nanocrystals from corncob for application as reinforcing agent in nanocomposites. *Ind. Crops Prod.*, **44**, 427–436.

135 Kumar, A., Singh Negi, Y.S., Choudhary, V., and Bhardwaj, N.K. (2014) Characterization of cellulose nanocrystals produced by acid-hydrolysis from sugarcane bagasse as agro-waste. *J. Mater. Phys. Chem.*, **2** (1), 1–8.

136 Sacui, I.A., Nieuwendaal, R.C., Burnett, D.J., Stranick, S.J., Jorfi, M., Weder, C., Foster, E.J., Olsson, R.T., and Gilman, J.W. (2014) Comparison of the properties of cellulose nanocrystals and cellulose nanofibrils isolated from bacteria, tunicate, and wood processed using acid, enzymatic, mechanical, and oxidative methods. *ACS Appl. Mater. Interfaces*, **6**, 6127–6138.

137 Lu, P. and Hsieh, Y.L. (2012) Preparation and characterization of cellulose nanocrystals from rice straw. *Carbohydr. Polym.*, **87**, 564–573.
138 Sheltami, R.M., Abdullah, I., Ahmad, I., Dufresne, A., and Kargarzadeh, H. (2012) Extraction of cellulose nanocrystals from mengkuang leaves (*Pandanus tectorius*). *Carbohydr. Polym.*, **88** (2), 772–779.
139 Rosli, N.A., Ahmad, I., and Abdullah, I. (2013) Isolation and characterization of cellulose nanocrystals from *Agave angustifolia* fiber. *Bioresources*, **8** (2), 1893–1908.
140 Oun, A.A. and Rhim, J.W. (2015) Effect of post-treatments and concentration of cotton linter cellulose nanocrystals on the properties of agar-based nanocomposite films. *Carbohydr. Polym.*, **134**, 20–29.
141 Lamaming, J., Hashim, R., Leh, C.P., and Sulaiman, O. (2015) Isolation and characterization of cellulose nanocrystals from parenchyma and vascular bundle of oil palm trunk (*Elaeis guineensis*). *Carbohydr. Polym.*, **134**, 534–540.
142 Jiang, F. and Hsieh, Y.L. (2015) Cellulose nanocrystal isolation from tomato peels and assembled nanofibers. *Carbohydr. Polym.*, **122**, 60–68.
143 Danial, W.H., Majid, Z.A., Muhid, M.N.M., Triwahyono, S., Bakar, M.B., and Ramli, Z. (2015) The reuse of wastepaper for the extraction of cellulose nanocrystals. *Carbohydr. Polym.*, **118**, 165–169.
144 Rhim, J.W., Reddy, J.P., and Luo, X. (2015) Isolation of cellulose nanocrystals from onion skin and their utilization for the preparation of agar-based bio-nanocomposites films. *Cellulose*, **22**, 407–420.
145 Cesar, N.R., Pereira-da-Silva, M.A., Botaro, V.R., and de Menezes, A.J. (2015) Cellulose nanocrystals from natural fiber of the macrophyte *Typha domingensis*: extraction and characterization. *Cellulose*, **22** (1), 449–460.
146 Ghahafarrokhi, I.S., Khodaiyan, F., Mousavi, M., and Yousefi, H. (2015) Preparation and characterization of nanocellulose from beer industrial residues using acid hydrolysis/ultrasound. *Fibers Polym.*, **16** (3), 529–536.
147 Lu, Q., Lin, W., Tang, L., Wang, S., Chen, X., and Huang, B. (2015) A mechanochemical approach to manufacturing bamboo cellulose nanocrystals. *J. Mater. Sci.*, **50**, 611–619.
148 Lee, S.Y., Mohan, D.J., Kang, I.A., Doh, G.H., Lee, S., and Han, S. (2009) Nanocellulose reinforced PVA composite films: effects of acid treatment and filler loading. *Fibers Polym.*, **10** (1), 77–82.
149 Liu, Y., Wang, H., Yu, G., Yu, Q., Li, B., and Mu, X. (2014) A novel approach for the preparation of nanocrystalline cellulose by using phosphotungstic acid. *Carbohydr. Polym.*, **110**, 415–422.
150 Tang, L., Huang, B., Ou, W., Chen, X., and Chen, Y. (2011) Manufacture of cellulose nanocrystals by cation exchange resin-catalyzed hydrolysis of cellulose. *Bioresour. Technol.*, **102**, 10973–10977.
151 Hamid, S.B.A., Zain, S.K., and Centi, G. (2015) Synergic effect of tungstophosphoric acid and sonication for rapid synthesis of crystalline nanocellulose. *Carbohydr. Polym.*, **138**, 349–355.
152 Kontturi, E., Meriluoto, A., and Nuopponen, M. (2012) Process for preparing micro-and nanocrystalline cellulose. US Patent 14/006,477, filed Mar. 21, 2012.

153 Liu, L., Sun, J., Cai, C., Shuhao Wang, S., Pei, H., and Zhang, J. (2009) Corn stover pretreatment by inorganic salts and its effects on hemicellulose and cellulose degradation. *Bioresour. Technol.*, **100** (23), 5865–5871.
154 Kamireddy, S.R., Li, J., Tucker, M., Degenstein, J., and Ji, Y. (2013) Effects and mechanism of metal chloride salts on pretreatment and enzymatic digestibility of corn stover. *Ind. Eng. Chem. Res.*, **52** (5), 1775–1782.
155 López-Linares, J.C., Romero, I., Moya, M., Cara, C., Ruiz, E., and Castro, E. (2013) Pretreatment of olive tree biomass with $FeCl_3$ prior enzymatic hydrolysis. *Bioresour. Technol.*, **128**, 180–187.
156 Zhang, Y., Li, Q., Su, J., Lin, Y., Huang, Z., Lu, Y., Sun, G., Yang, M., Huang, A., and Hu, H. (2015) A green and efficient technology for the degradation of cellulosic materials: structure changes and enhanced enzymatic hydrolysis of natural cellulose pretreated by synergistic interaction of mechanical activation and metal salt. *Bioresour. Technol.*, **177**, 176–181.
157 Li, J., Zhang, X., Zhang, M., Xiu, H., and He, H. (2015) Ultrasonic enhance acid hydrolysis selectivity of cellulose with HCl–$FeCl_3$ as catalyst. *Carbohydr. Polym.*, **117**, 917–922.
158 Lu, Q., Tang, L., Lin, F., Wang, S., Chen, Y., Chen, X., and Huang, B. (2014) Preparation and characterization of cellulose nanocrystals via ultrasonication-assisted $FeCl_3$-catalyzed hydrolysis. *Cellulose*, **21** (5), 3497–3506.
159 Hamid, S.B.A., Chowdhury, Z.Z., and Karim, M.Z. (2014) Catalytic extraction of microcrystalline cellulose (MCC) from elaeis guineensis using central composite design (CCD). *Bioresources*, **9** (4), 7403–7426.
160 Yahya, M., Lee, H.V., and Hamid, S.B.A. (2015) Preparation of nanocellulose via transition metal salt catalyzed hydrolysis pathway. *Bioresources*, **10** (4), 7627–7639.
161 Karim, M.Z., Chowdhury, Z.Z., Hamid, S.B.A., and Ali, M.E. (2014) Statistical optimization for acid hydrolysis of microcrystalline cellulose and its physiochemical characterization by using metal ion catalyst. *Materials*, **7**, 6982–6999.
162 Man, Z., Muhammad, N., Sarwono, A., Bustam, M.A., Kumar, M.V., and Rafiq, S. (2011) Preparation of cellulose nanocrystals using an ionic liquid. *J. Polym. Environ.*, **19** (3), 726–731.
163 Abbott, A.P., Capper, G., Davies, D.L., Rasheed, R.K., and Tambyrajah, V. (2003) Novel solvent properties of choline chloride/urea mixtures. *Chem. Commun.*, **1**, 70–71.
164 Abbott, A.P., Harris, R.C., Ryder, K.S., D'Agostino, C., Gladden, L.F., and Mantle, M.D. (2011) Glycerol eutectics as sustainable solvent systems. *Green Chem.*, **13**, 82–90.
165 De Santi, V., Cardellini, F., Brinchi, L., and Germani, R. (2012) Novel Bronsted acidic deep eutectic solvents as reaction media for esterification of carboxylic acid with alcohols. *Tetrahedron Lett.*, **53** (38), 5151–5155.
166 Siqueira, G., Tapin-Lingua, S., Bras, J., da Silva Perez, D., and Dufresne, A. (2010) Morphological investigation of nanoparticles obtained from combined mechanical shearing, and enzymatic and acid hydrolysis of sisal fibers. *Cellulose*, **17**, 1147–1158.

167 Filson, P.B., Dawson-Andoh, B., and Schwegler-Berry, D. (2009) Enzymatic-mediated production of cellulose nanocrystals from recycled pulp. *Green Chem.*, **11** (11), 1808–1814.
168 Hirota, M., Tamura, N., Saito, T., and Isogai, A. (2010) Water dispersion of cellulose II nanocrystals prepared by TEMPO-mediated oxidation of mercerized cellulose at pH 4.8. *Cellulose*, **17**, 279–288.
169 Li, Y. *et al.* (2016) Facile extraction of cellulose nanocrystal from wood using ethanol and peroxide solvothermal pretreatment followed by ultra sonic nanofibrillation. *Green Chem.*, **18**, 1010–1018.
170 Ono, H., Matsui, T., and Miyamoto, I. (2003) Cellulose dispersion. US Patent 6, 541, 627.
171 Zhang, J., Elder, T.J., Pu, Y., and Ragauskas, A.J. (2007) Facile synthesis of spherical cellulose nanoparticles. *Carbohydr. Polym.*, **69** (3), 607–611.
172 Wang, N., Ding, E., and Cheng, R. (2007) Thermal degradation behavior of spherical cellulose nanocrystals with sulfate groups. *Polymer*, **48** (12), 3486–3493.
173 Wang, N., Ding, E., and Cheng, R. (2008) Preparation and liquid crystalline properties of spherical cellulose nanocrystals. *Langmuir*, **24**, 5–8.
174 Yang, D., Peng, X.W., Zhong, L.X., Cao, X.F., Chen, W., and Sun, R.C. (2013) Effects of pretreatments on crystalline properties and morphology of cellulose nanocrystals. *Cellulose*, **20**, 2427–2437.
175 Lim, Y.-M., Gwon, H.-J., Jeun, J.P., and Nho, Y.-C. (2010) in *Nanofibers* (ed. A. Kumar), INTECH Open Access Publisher, Rijeka, Croatia, pp. 179–188.
176 Frey, M.W. (2008) Electrospinning cellulose and cellulose derivatives. *Polym. Rev.*, **48** (2), 378–391.
177 Kulpinski, P. (2005) Cellulose nanofibers prepared by the *N*-methylmorpholine-*N*-oxide method. *J. Appl. Polym. Sci.*, **98** (4), 1855–1859.
178 Qi, H., Sui, X., Yuan, J., Wei, Y., and Zhang, L. (2010) Electrospinning of cellulose-based fibers from NaOH/urea aqueous system. *Macromol. Mater. Eng.*, **295** (8), 695–700.
179 Frey, M. and Joo, Y. (2004) Cellulose solution in novel solvent and electrospinning thereof. US Patent 20050247236, filed Apr. 29, 2004 and issued Nov. 10, 2005.
180 Christoforou, T. and Doumanidis, C. (2010) Biodegradable cellulose acetate nanofiber fabrication via electrospinning. *J. Nanosci. Nanotechnol.*, **10** (9), 6226–6233.
181 Han, S.O., Youk, J.H., Min, K.D., Kang, Y.O., and Park, W.H. (2008) Electrospinning of cellulose acetate nanofibers using a mixed solvent of acetic acid/water: effects of solvent composition on the fiber diameter. *Mater. Lett.*, **62** (4–5), 759–762.
182 van den Berg, O., Capadona, J.R., and Weder, C. (2007) Preparation of homogeneous dispersions of tunicate cellulose whiskers in organic solvents. *Biomacromolecules*, **8** (4), 1353–1357.
183 Mihranyan, A. (2011) Cellulose from cladophorales green algae: from environmental problem to high-tech composite materials. *J. Appl. Polym. Sci.*, **119** (4), 2449–2460.

184 Ek, M., Gellerstedt, G., and Henriksson, G. (2009) *Pulp and Paper Chemistry and Technology*, Pulping Chemistry and Technology, vol. **2**, Walter de Gruyter, Berlin.

185 Chaker, A., Alila, S., Mutjé, P., Vilar, M.R., and Boufi, S. (2013) Key role of the hemicellulose content and the cell morphology on the nanofibrillation effectiveness of cellulose pulps. *Cellulose*, **20**, 2863–2875.

186 Fritzvold, B.H. (1981) Method for bleaching pulp with ozone. US Patent 4,902,381, filed Jul. 13, 1979 and issued Jul. 14, 1981.

187 Fritzvold, B.H. and Soteland, N. (1984) Method for bleaching oxygen delignified cellulose containing pulp with ozone and peroxide. US Patent 4,450,044, field Jul. 19, 1982 and issued May 22, 1984.

188 Yuan, Z., Ni, Y., and Van Heiningen, A. (1997) Kinetics of peracetic acid decomposition: part I: spontaneous decomposition at typical pulp bleaching conditions. *Can. J. Chem. Eng.*, **75** (1), 37–41.

189 Bhatnagar, A. and Sain, M. (2005) Processing of cellulose nanofiber reinforced composites. *J. Reinf. Plast. Compos.*, **24**, 1259–1268.

190 Wang, B., Sain, M., and Oksman, K. (2007) Study of structural morphology of hemp fiber from the micro to the nanoscale. *Appl. Compos. Mater.*, **14**, 89–103.

191 Janardhnan, S. and Sain, M. (2006) Isolation of cellulose microfibrils–An enzymatic approach. *Bioresources*, **1**, 176–188.

192 Zhang, Y.H.P., Himmel, M.E., and Mielenz, J.R. (2006) Outlook for cellulase improvement: screening and selection strategies. *Biotechnol. Adv.*, **24**, 452–481.

193 Henriksson, M., Henriksson, G., Berglund, L.A., and Lindström, T. (2007) An environmentally friendly method for enzyme-assisted preparation of microfibrillated cellulose (MFC) nanofibers. *Eur. Polym. J.*, **43**, 3434–3441.

194 Pääkkö, M., Ankerfors, M., Kosonen, H., Nykanen, A., Ahola, S., Osteberg, M., Ruokolainen, J., Laine, J., Larsson, P.T., Ikkala, O., and Lindström, T. (2007) Enzymatic hydrolysis combined with mechanical shearing and high-pressure homogenization for nanoscale cellulose fibrils and strong gels. *Biomacromolecules*, **8** (6), 1934–1941.

195 Pinkert, A., Marsh, K.N., Pang, S., and Staiger, M.P. (2009) Ionic liquids and their interaction with cellulose. *Chem. Rev.*, **109** (12), 6712–6728.

196 Zhu, S.D., Wu, Y.X., Chen, Q.M., Yu, Z.N., Wang, C.W., Jin, S.W., Ding, Y., and Wu, G. (2006) Dissolution of cellulose with ionic liquids and its application: a mini-review. *Green Chem.*, **8** (4), 325–327.

197 Li, J., Wei, X., Wang, Q., Chen, J., Chang, G., Kong, L., Su, J., and Liu, Y. (2012) Homogeneous isolation of nanocellulose from sugarcane bagasse by high pressure homogenization. *Carbohydr. Polym.*, **90**, 1609–1613.

198 Tan, X.Y., Hamid, S.B.A., and Lai, C.W. (2015) Preparation of high crystallinity cellulose nanocrystals (CNCs) by ionic liquid solvolysis. *Biomass Bioenergy*, **8**, 584–591.

199 Gindl, W. and Keckes, J. (2005) All-cellulose nanocomposite. *Polymer*, **46** (23), 10221–10225.

200 Kilpeläinen, I., Xie, H., King, A., Granstrom, M., Heikkinen, S., and Argyropoulos, D.S. (2007) Dissolution of wood in ionic liquids. *J. Agric. Food Chem.*, **55** (22), 9142–9148.
201 Sui, X., Yuan, J., Yuan, W., and Zhou, M. (2008) Preparation of cellulose nanofibers/nanoparticles via electrospray. *Chem. Lett.*, **37** (1), 114–115.
202 Kadokawa, J., Murakami, M., and Kaneko, Y. (2008) A facile method for preparation of composites composed of cellulose and a polystyrene-type polymeric ionic liquid using a polymerizable ionic liquid. *Compos. Sci. Technol.*, **68** (2), 493–498.
203 Isogai, A., Saito, T., and Fukuzumi, H. (2011) TEMPO-oxidized cellulose nanofibers. *Nanoscale*, **3** (1), 71–85.
204 Bragd, P., Van Bekkum, H., and Besemer, A. (2004) TEMPO-mediated oxidation of polysaccharides: survey of methods and applications. *Top. Catal.*, **27** (1–4), 49–66.
205 Saito, T. and Isogai, A. (2004) TEMPO-mediated oxidation of native cellulose. The effect of oxidation conditions on chemical and crystal structures of the water-insoluble fractions. *Biomacromolecules*, **5** (5), 1983–1989.
206 Shibata, I. and Isogai, A. (2003) Depolymerization of cellouronic acid during TEMPO-mediated oxidation. *Cellulose*, **10** (2), 151–158.
207 Besbes, I., Alila, S., and Boufi, S. (2011) Nanofibrillated cellulose from TEMPO-oxidized eucalyptus fibres: effect of the carboxyl content. *Carbohydr. Polym.*, **84** (3), 975–983.
208 Besbes, I., ReiVilar, M., and Boufi, S. (2011) Nanofibrillated cellulose from alfa, eucalyptus and pine fibres: preparation, characteristics and reinforcing potential. *Carbohydr. Polym.*, **86**, 1198–1206.
209 Shinoda, R., Saito, T., Okita, Y., and Isogai, A. (2012) Relationship between length and degree of polymerization of TEMPO-oxidized cellulose nanofibrils. *Biomacromolecules*, **13**, 842–849.
210 Soni, B., Hassan, E.B., and Mahmoud, B. (2015) Chemical isolation and characterization of different cellulose nanofibers from cotton stalks. *Carbohydr. Polym.*, **134**, 581–589.
211 Qin, Z.Y., Tong, G., Chin, Y.C.F., and Zhou, J.C. (2011) Preparation of ultrasonic-assisted high carboxylate content cellulose nanocrystals by TEMPO oxidation. *Bioresources*, **6** (2), 1136–1146.
212 Carlsson, D.O., Lindh, J., Nyholm, L., Stromme, M., and Mihranyan, A. (2014) Cooxidant-free TEMPO-mediated oxidation of highly crystalline nanocellulose in water. *RSC Adv.*, **4** (94), 52289–52298.
213 Tejado, A., Alam, M.N., Antal, M., Yang, H.P., and van de Ven, T.G.M. (2012) Energy requirements for the disintegration of cellulose fibers into cellulose nanofibers. *Cellulose*, **19** (3), 831–842.
214 Cristóbal, C., Encarnación, R., Mercedes, B., Paloma, M., José, M.N., and Eulogio, C. (2008) Production of fuel ethanol from steam-explosion pretreated olive tree pruning. *Fuel*, **87** (6), 692–700.
215 Deepa, B., Abraham, E., Cherian, B.M., Bismarck, A., Blaker, J.J., Pothan, L.A., Leão, A.L., de Souza, S.F., and Kottaisamy, M. (2011) Structure, morphology and thermal characteristics of banana nanofiber obtained by steam explosion. *Bioresour. Technol.*, **102** (2), 1988–1997.

216 Kessler, R., Becker, U., Kohler, R., and Goth, B. (1998) Steam explosion of flax—a superior technique for upgrading fibre value. *Biomass Bioenergy*, **14** (3), 237–249.

217 Jeoh, T. and Agblevor, F. (2001) Characterization and fermentation of steam exploded cotton gin waste. *Biomass Bioenergy*, **21** (2), 109–120.

218 Kaushik, A., Singh, M., and Verma, G. (2010) Green nanocomposites based on thermoplastic starch and steam exploded cellulose nanofibrils from wheat straw. *Carbohydr. Polym.*, **82** (2), 337–345.

219 Shao, S., Wen, G., and Jin, Z. (2008) Changes in chemical characteristics of bamboo (*Phyllostachys pubescens*) components during steam explosion. *Wood Sci. Technol.*, **42** (6), 439–451.

220 Cherian, B.M., Leão, A.L., de Souza, S.F., Thomas, S., Pothan, L.A., and Kottaisamy, M. (2010) Isolation of nanocellulose from pineapple leaf fibres by steam explosion. *Carbohydr. Polym.*, **81** (3), 720–725.

221 Boufi, S. (2014) in *Biomass and Bioenergy* (eds K.R. Hakeem, M. Jawaid, and U. Rashid), Springer, Cham (ZG), Switzerland, pp. 267–305.

222 Aulin, C., Ahola, S., Josefsson, P., Nishino, T., Hirose, Y., Österberg, M., and Wågberg, L. (2009) Nanoscale cellulose films with different crystallinities and mesostructures: their surface properties and interaction with water. *Langmuir*, **25** (13), 7675–7685.

223 Taipale, T., Österberg, M., Nykänen, A., Ruokolainen, J., and Laine, J. (2010) Effect of microfibrillated cellulose and fines on the drainage of kraft pulp suspension and paper strength. *Cellulose*, **17** (5), 1005–1020.

224 Tingaut, P., Zimmermann, T., and Lopez-Suevos, F. (2009) Synthesis and characterization of bionanocomposites with tunable properties from poly (lactic acid) and acetylated microfibrillated cellulose. *Biomacromolecules*, **11** (2), 454–464.

225 Qua, E.H., Hornsby, P.R., Sharma, H.S.S., Lyons, G., and McCall, R.D. (2009) Preparation and characterization of poly(vinyl alcohol) nanocomposites made from cellulose nanofibers. *J. Appl. Polym. Sci.*, **113** (4), 2238–2247.

226 Spence, K.L., Venditti, R.A., Rojas, O.J., Habibi, Y., and Pawlak, J.J. (2011) A comparative study of energy consumption and physical properties of microfibrillated cellulose produced by different processing methods. *Cellulose*, **18**, 1097–1111.